Accelerator Physics Issues at LHC & Beyond
Part II

Frank Zimmermann, CERN, SL/AP

(A) Past and Future

(B) The Large Hadron Collider (LHC)

- parameters, magnets, beam-beam effects, pre-injectors, ion collisions,...
- A new phenomenon: Electron Cloud (today)

(C) LHC Upgrades, VLHC-I and II (today)

Electron Cloud

Observed with the LHC beam:

1999 SPS, 2000 PS, 2000 PS-SPS transfer line

primary e− generated by photoemission or gas ionization; their number amplifies along a bunch train due to beam-induced multipacting

(1) Build Up, Saturation, Decay

(2) Wake Fields and Instabilities

(3) Heat Load

(4) LHC Approach

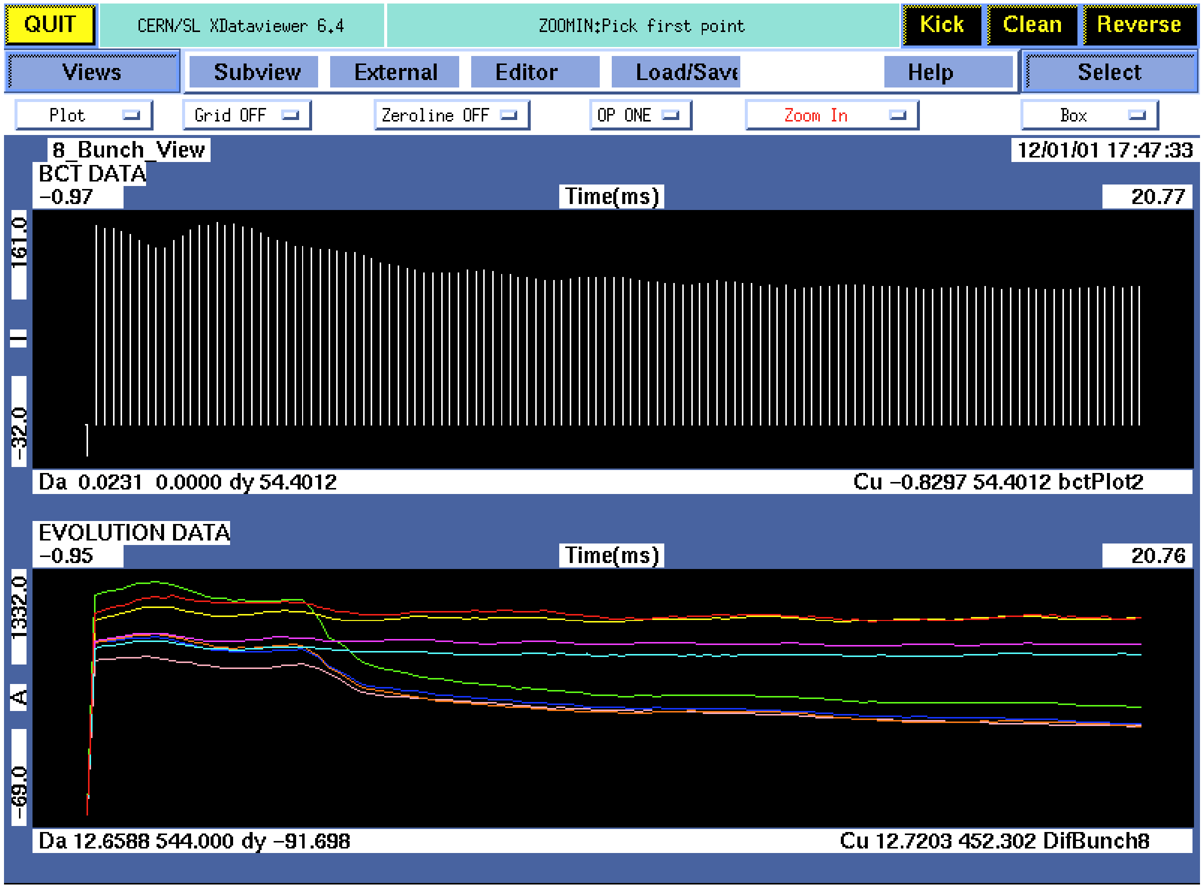

Da 0.0231 0.0000 dy 54.4012

Cu -0.8297 54.4012 bctPlot2

Da 12.6588 544.000 dy -91.698

Cu 12.7203 452.302 DifBunch8

Intensity of 72-bunch LHC beam in SPS vs. time. Batch intensity (top) and bunch intensity for the first 4 bunches and last 4 bunches (where losses are visible after about 5 ms) of the batch (bottom). (Courtesy G. Arduini, 2001).

Build Up, Saturation, Decay

e^- production mechanisms:

- residual gas ionization;
  typical rate $d^2\lambda_e/(ds\ dt) \approx 5 \times 10^{11} \mathrm{e}^- \ \mathrm{m}^{-1}\mathrm{s}^{-1}$
- synchrotron radiation and photo-emission;
  typical rate $d^2\lambda_e/(ds\ dt) \approx 5 \times 10^{18} \ \mathrm{e}^- \ \mathrm{m}^{-1}\mathrm{s}^{-1}$
- secondary emission: (1) true secondaries & (2) elastically reflected or rediffused; →
  exponential growth

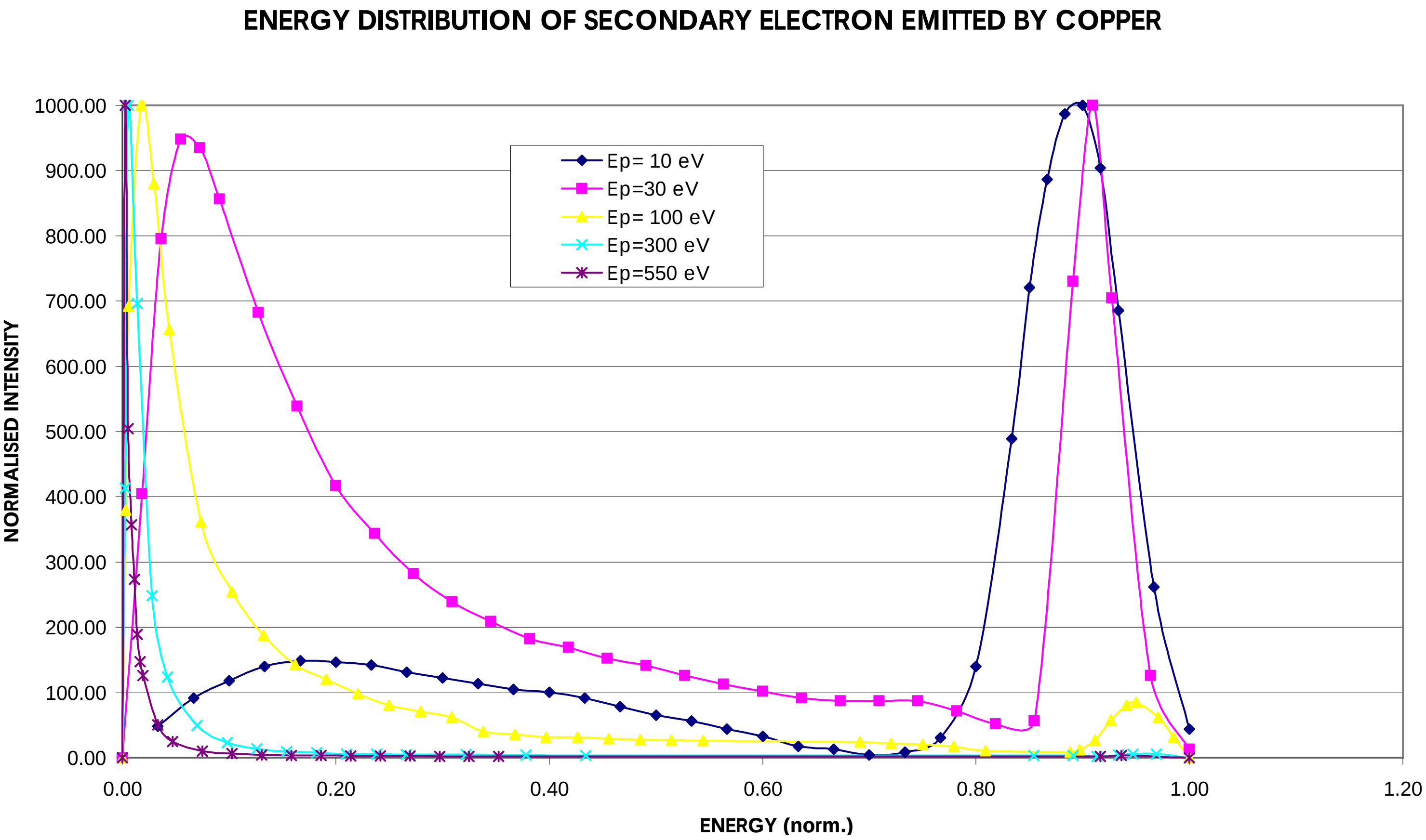

Normalized secondary electron energy distribution for conditioned copper, revealing three components: true secondaries ($E \ll E_p$), elastically scattered ($E \approx E_p$) and rediffused (in between). [N. Hilleret, 2001]

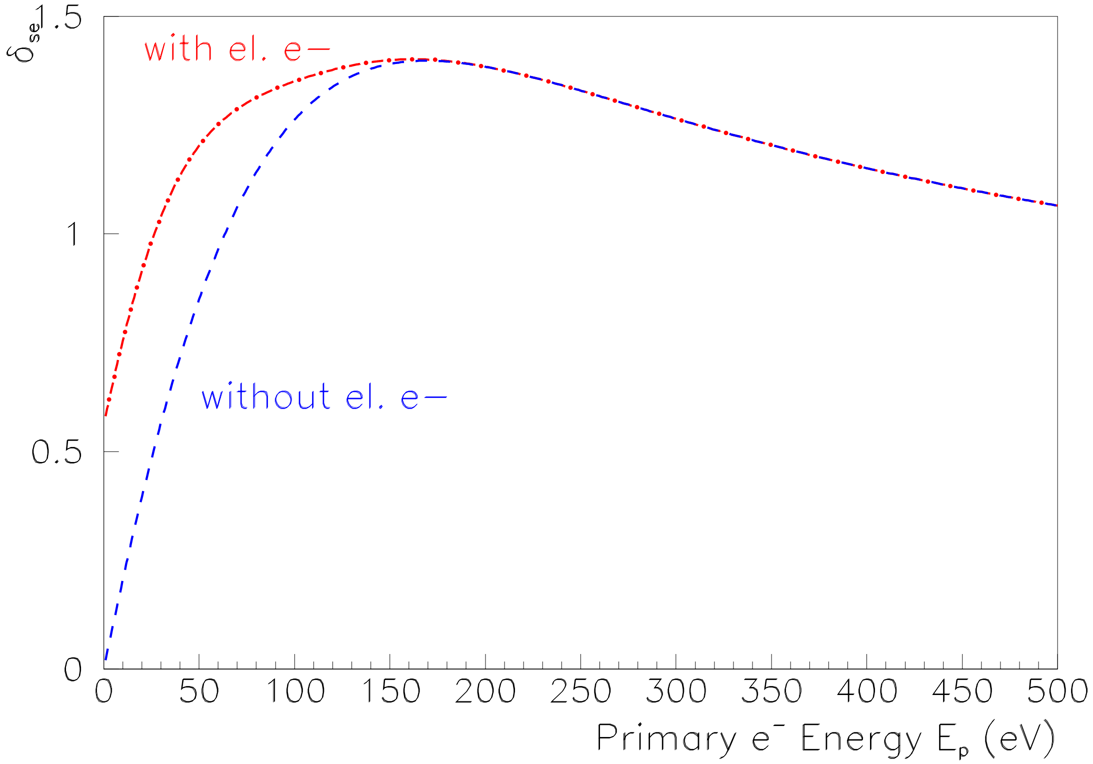

Secondary emission yield for perpendicular incidence vs. primary electron energy with and w/o elastically scattered electrons. Parametrization based on measurements for LHC prototype chamber. [Ian Collins, 2000]

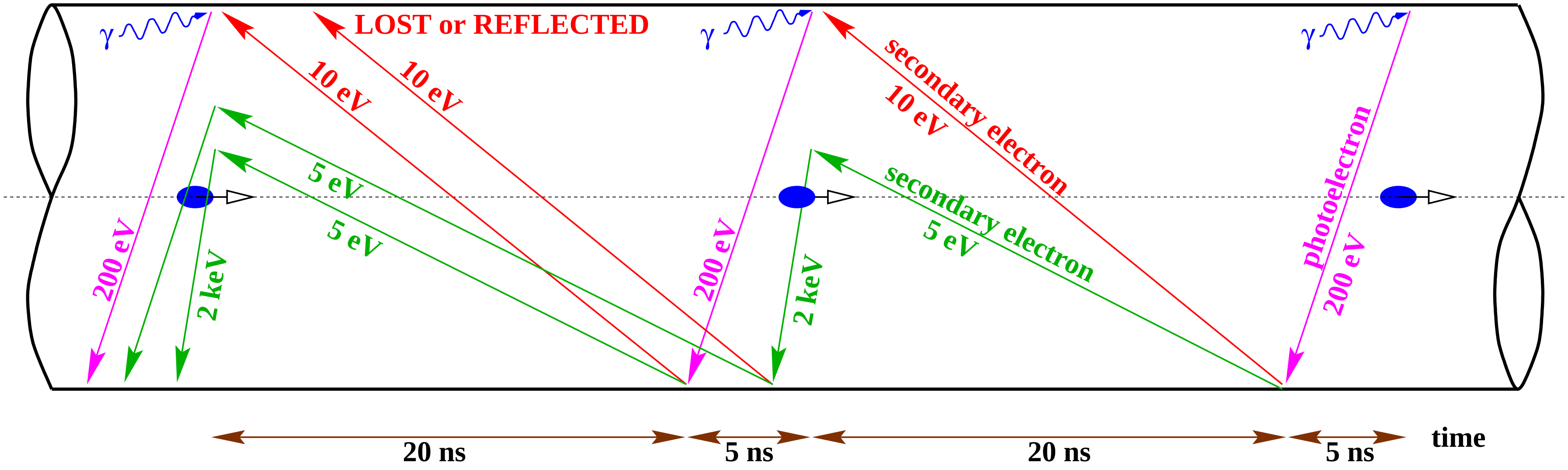

Schematic of electron-cloud build up in the LHC beam pipe. [Courtesy Francesco Ruggiero]

Proper multipacting: $n_{\min} \equiv \frac{h_y^2}{N_b r_e L_{\rm sep}} = 1$

accelerator	PEP-II	KEKB	PS	SPS	LHC	PSR	SNS
species	e^+	e^+	p	p	p	p	p
population N_b $[10^{10}]$	10	3.3	10	10	10	5000	1000
spacing L_{sep} [m]	2.5	2.4	7.5	7.5	7.5	(108)	(248
bunch length σ_z [m]	0.013	0.004	0.3	0.3	0.077	25	30
h. beam size σ_x [mm]	1.4	0.42	2.4	3	0.3	25	0.6
v. beam size σ_y [mm]	0.2	0.06	1.3	2.3	0.3	7.5	0.6
ch. $\frac{1}{2}$ size h_x [mm]	25	47	70	70	22	50	100
ch. $\frac{1}{2}$ size h_y [mm]	25	47	35	22.5	18	50	100
circumf. C [km]	2.2	3.0	0.63	6.9	27	0.09	0.22
beta function β	18	15	15	40	80	5	6
parameter n_{min}	1	10	0.58	0.24	0.15	0.0002	0.000

Simulation of Cloud Build Up (Schematic)

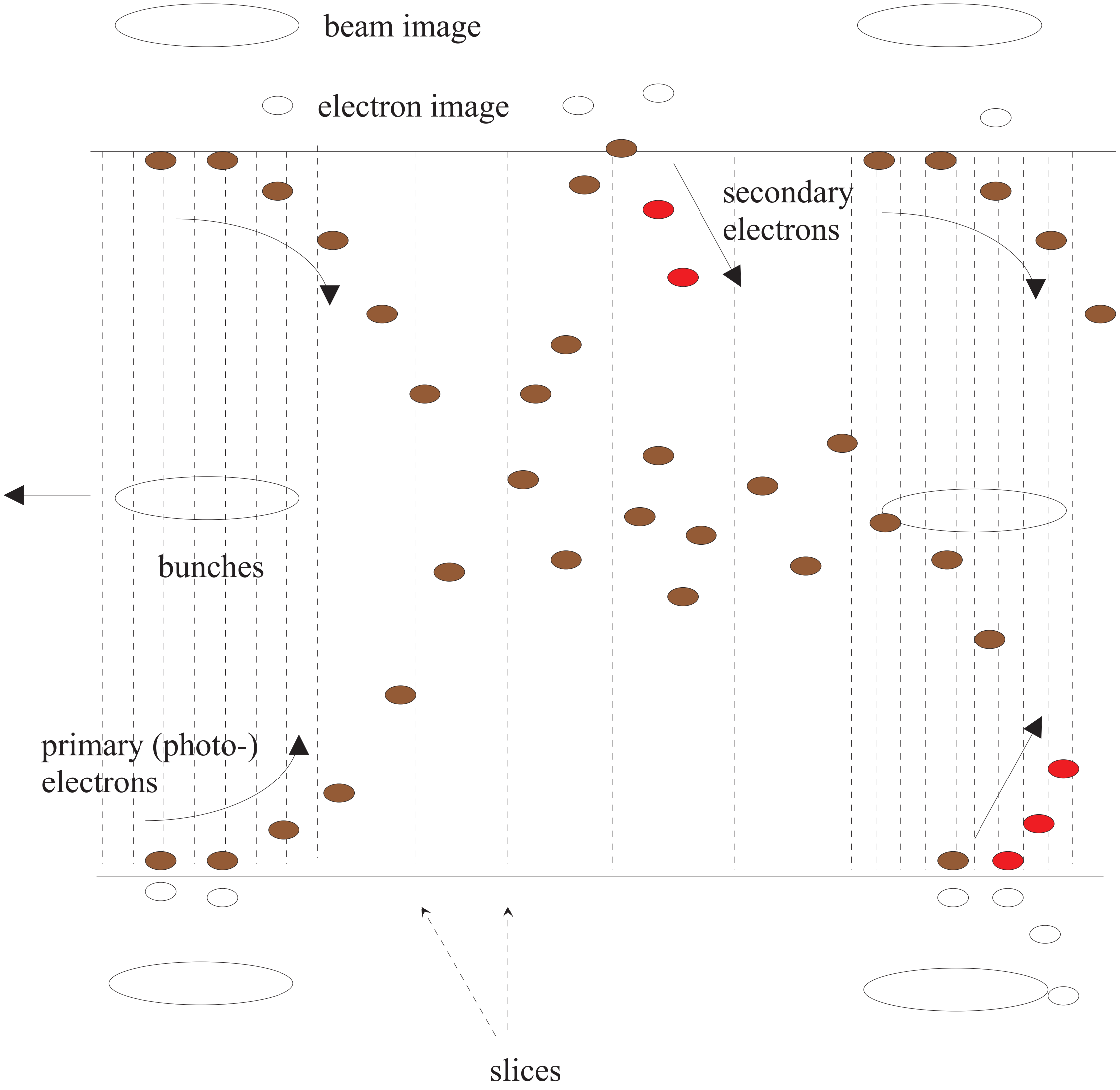

indicators of e^- build up

(1) nonlinear pressure rise → ρ_e

(2) pick ups or dedicated e^- monitors → ρ_e

(3) tune shift along the train → ρ_e

(4) beam-size blow up along the train

(5) luminosity drop

example: magnitude of e^- cloud in the SPS

(1) from pressure rise [O. Gröbner] :

pressure balance reads $S_{\rm eff} P/(k_B T) = Q$, where $S_{\rm eff}$ pumping speed in volume per meter per second, $Q = \alpha d\dot{\lambda}_e/ds$ total flux of molecules per unit length (α: desorption yield per electron) and $P = k_B T N/V$.

$$\frac{d\lambda_e}{ds} = \frac{T_{rev}}{\alpha k_B T} S_{\rm eff} P$$

With $P = 100$ nTorr, $\alpha \approx 0.1$ and $S_{\rm eff} \approx 20$ l s^{-1} m^{-1}:

$$\frac{d\lambda_e}{ds} \approx 10^{10} \frac{\rm electrons}{\rm bunch - train\ meter}$$

(2) from damper pick-up measurements [W. Hoefle]:

a few 10^8 electrons per bunch passage are deposited on the pick-up; this amounts to $10^9 - 10^{10}$ per train, or, with an effective pick-up length of about 10 cm,

$$\frac{d\lambda_e}{ds} \approx 10^{10} \frac{\text{electrons}}{\text{bunch} - \text{train meter}}$$

The two estimates are consistent.

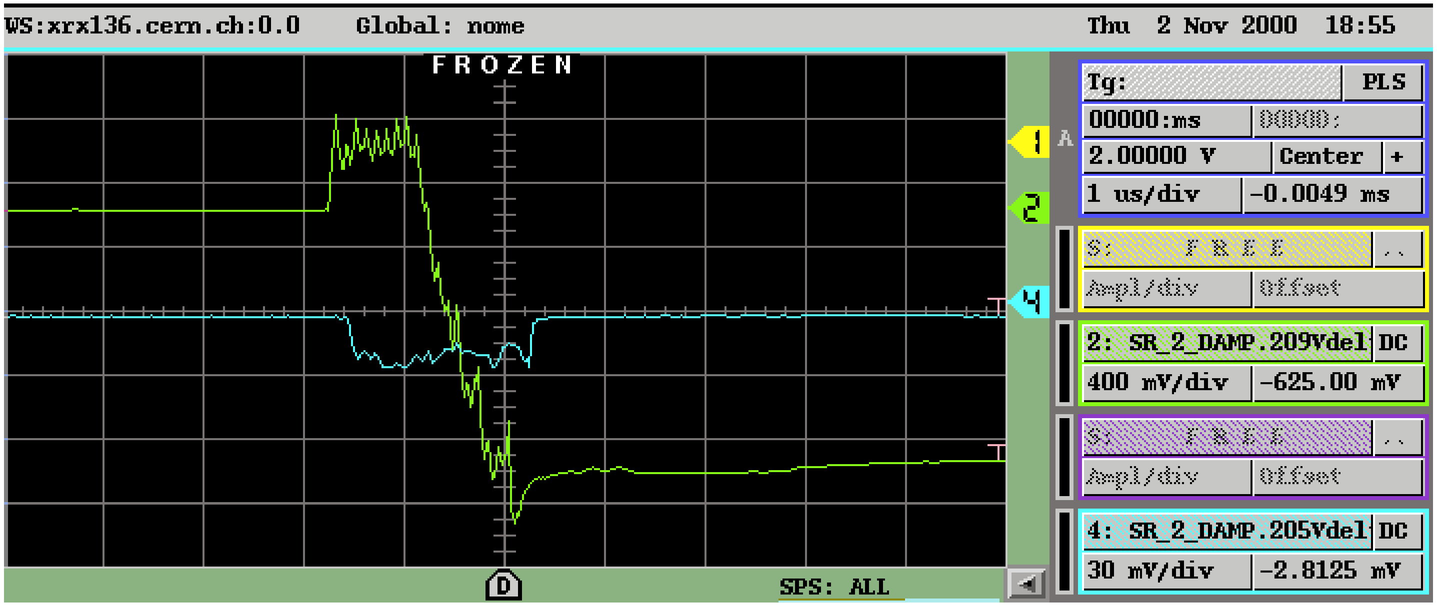

WS:xrx136.cern.ch:0.0 Global: none Thu 2 Nov 2000 18:55

Tg: PLS

00000:ms 00000:

2.00000 V Center +

1 us/div -0.0049 ms

S: FREE ..

Ampl/div Offset

2: SR_2_DAMP.209Vdel DC

400 mV/div -625.00 mV

S: FREE ..

Ampl/div Offset

4: SR_2_DAMP.205Vdel DC

30 mV/div -2.8125 mV

SPS: ALL

Sum and difference signal on damper pick-up during the passage of an LHC batch in the SPS (1μs/div). (Courtesy W. Hofle, 2001).

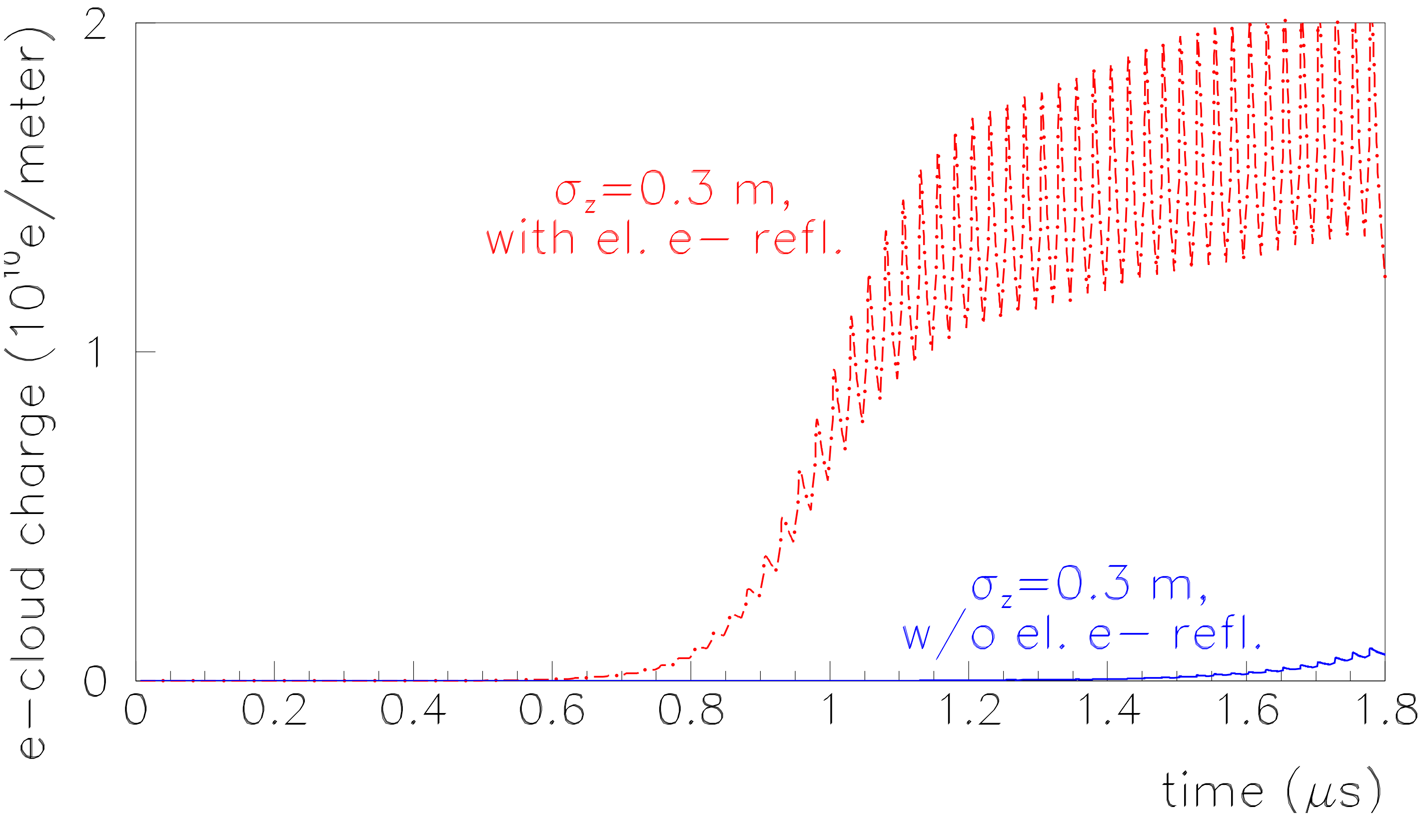

Simulated electron-cloud build up for an SPS dipole chamber, with and without elastic electron reflection. Saturation at

$\lambda_{e,\mathrm{sat}} \sim N_b/L_{\mathrm{sep}} \approx 1.3 \times 10^{10}\ \mathrm{m}^{-1}$ → 'neutralization' density

$\rho_{\mathrm{sat}} \approx N_b/(\pi h_x h_y L_{\mathrm{sep}}) \approx 3 \times 10^{12}\ \mathrm{m}^{-3}$.

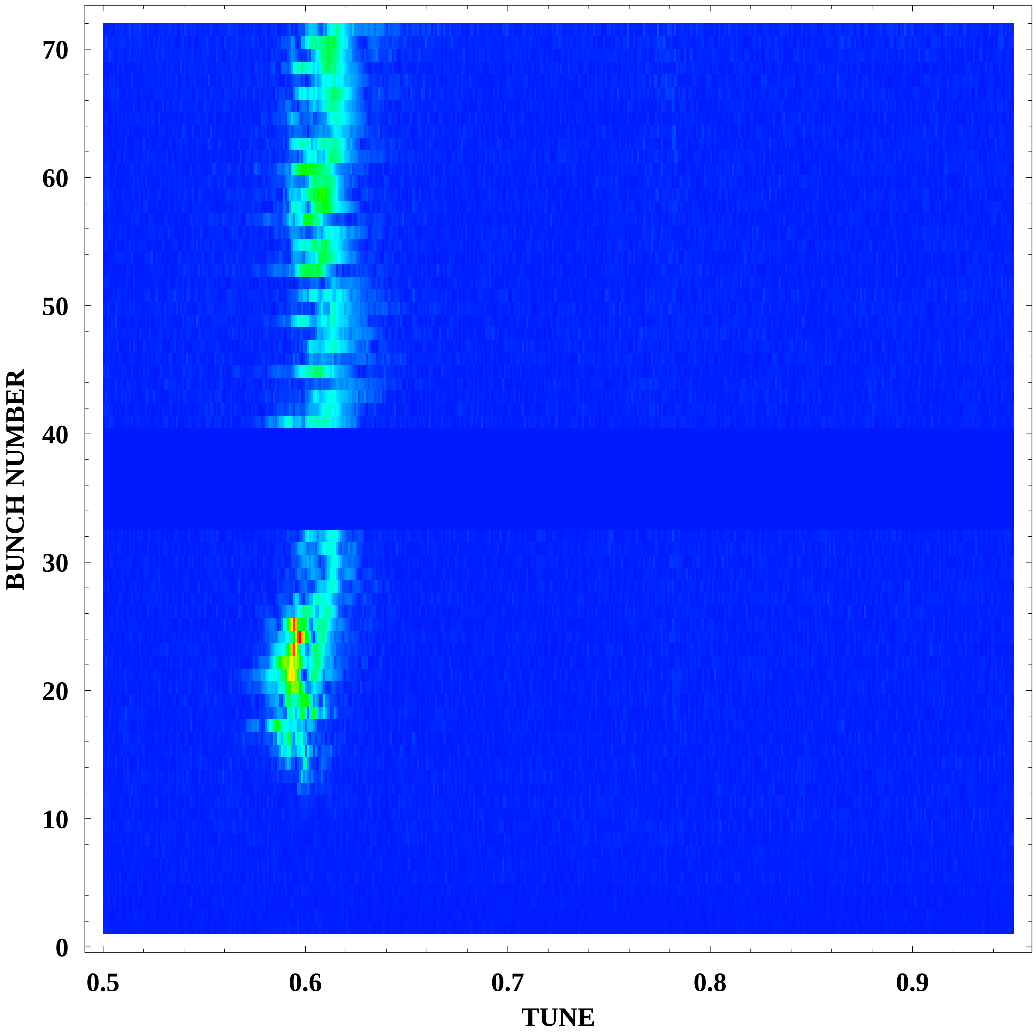

Fourier spectrum of the vertical oscillations of the LHC-beam bunch centroids as a function of bunch number

Wake Fields and Instability due to Electron Cloud

- Multi-Bunch Instability
- Coherent and Incoherent Tune Shift, etc.
- Single-Bunch Instability

  strong head-tail (TMCI), regular head-tail,
  transverse & longitudinal wakes,
  potential-well distortion

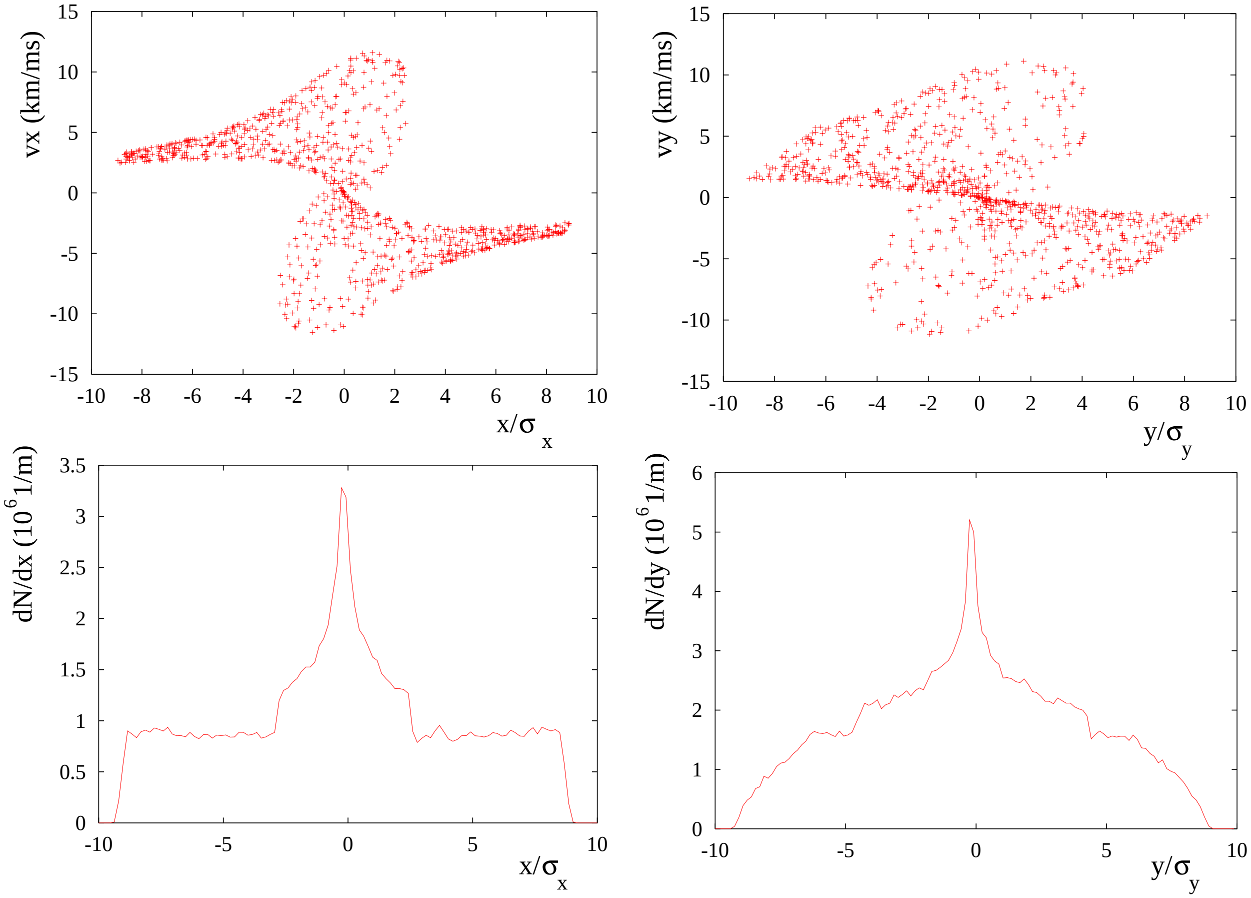

Snapshots of the horizontal and vertical electron phase space (top) and their projections onto the position axes (bottom). (Courtesy G. Rumolo, 2001).

adiabatic trapping (B. Richter, SLAC, March 2000)

WKB approximation → adiabaticity condition

$$A \equiv \sigma_z \omega_{e,y} \sqrt{8e}/c \gg 1$$

where $e = 2.718\ldots$

$A \approx 10$ for KEKB, PEP-II, PS, SPS, LHC!

Single-Bunch Instability

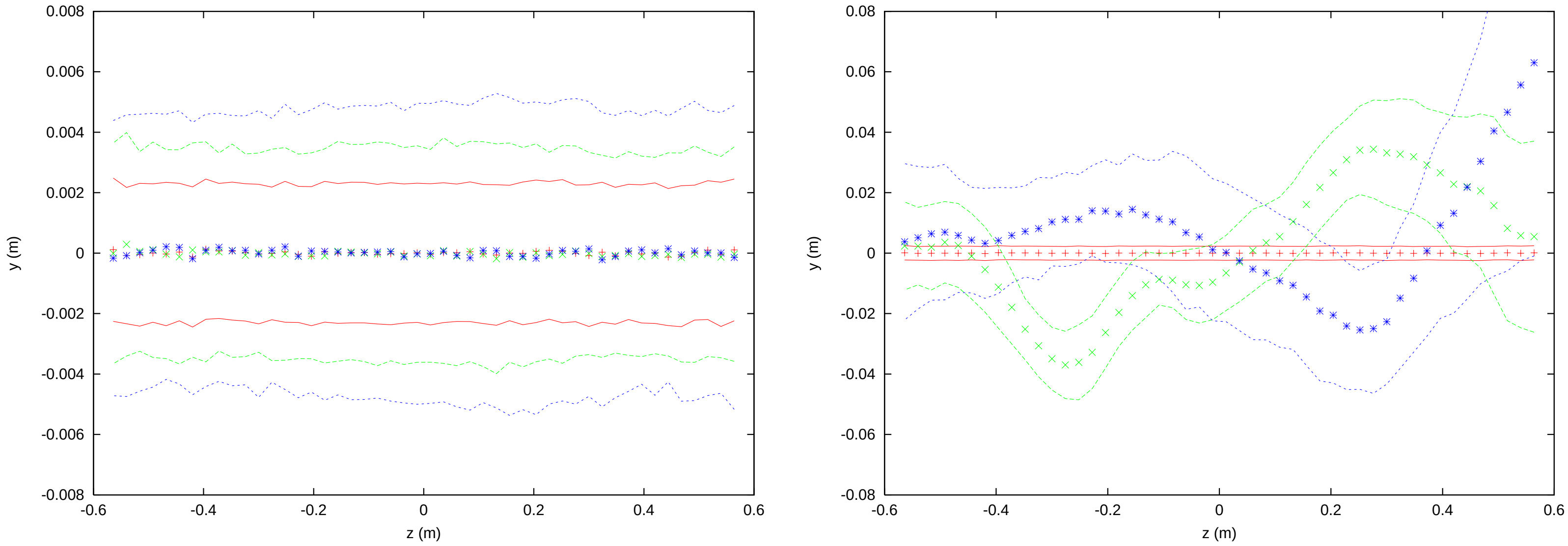

Simulated bunch shape after 0, 250 and 500 turns (centroid and rms beam size shown) in the CERN SPS with an e$^-$ cloud density of $\rho_e = 10^{12}$ m^{-3}, without (left) and with (right) proton space charge (Courtesy G. Rumolo).

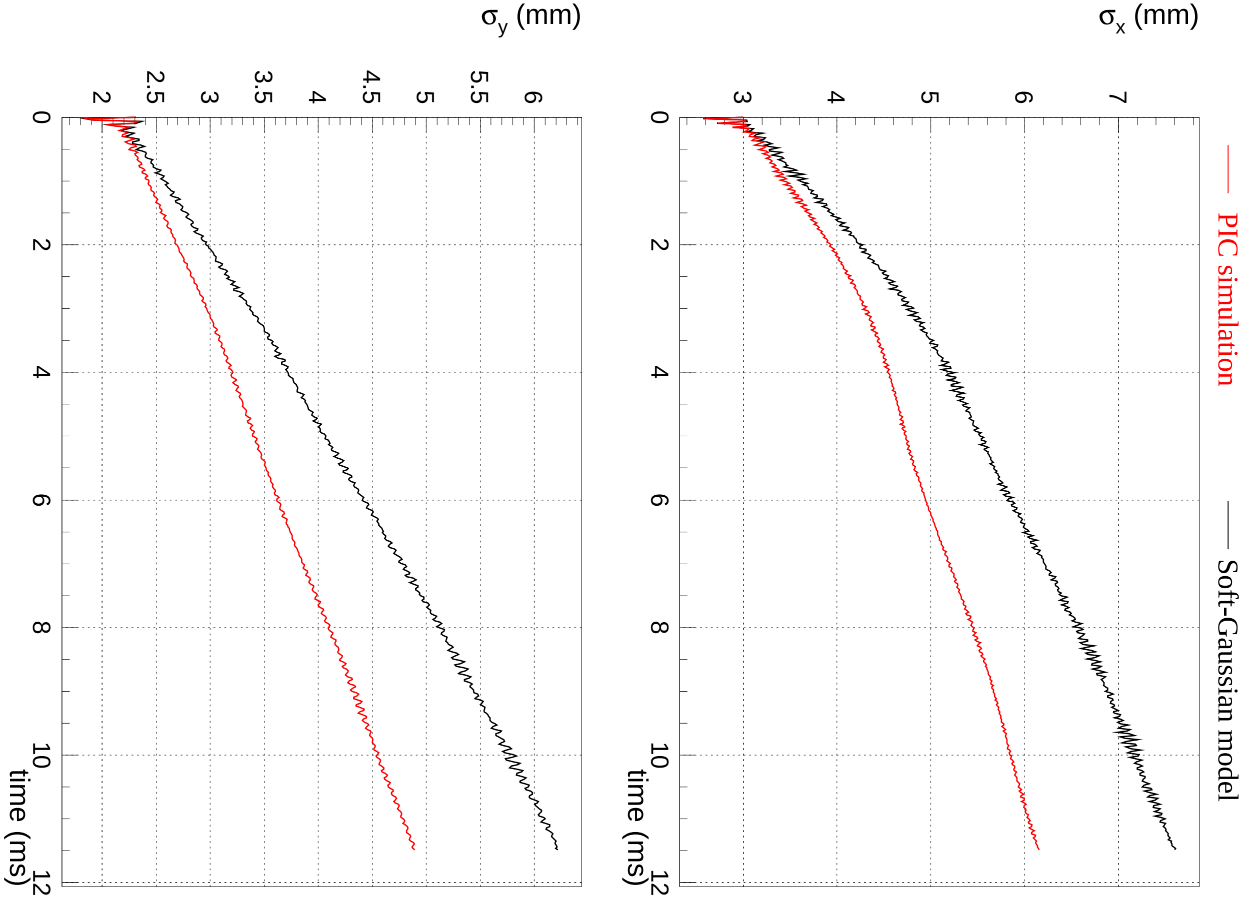

Beam size evolution for an SPS bunch interacting with an electron cloud as predicted by different simulation approaches. (Courtesy G. Rumolo, 2001).

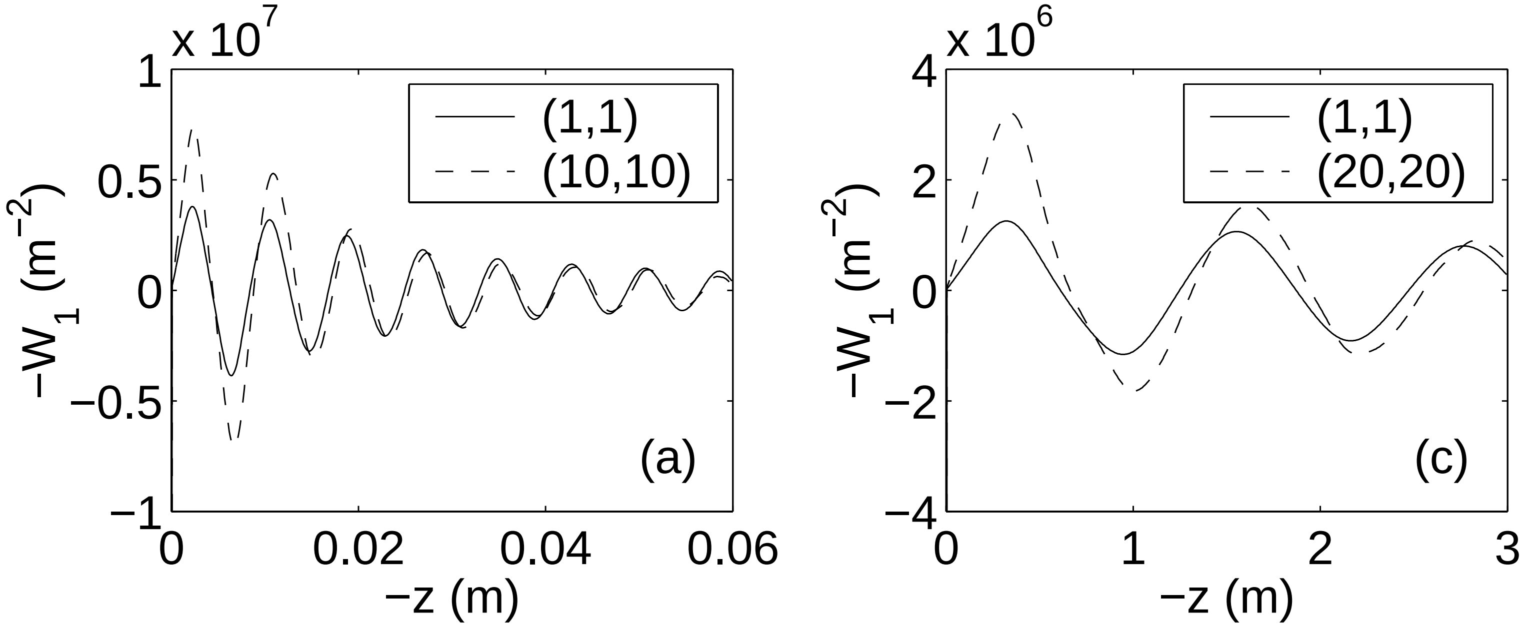

Wake force W_1 induced by an electron cloud; each line represents a different cloud size. Left: KEKB; right: SPS. [K. Ohmi et al., HEACC'01]. (Courtesy K. Ohmi, 2001).

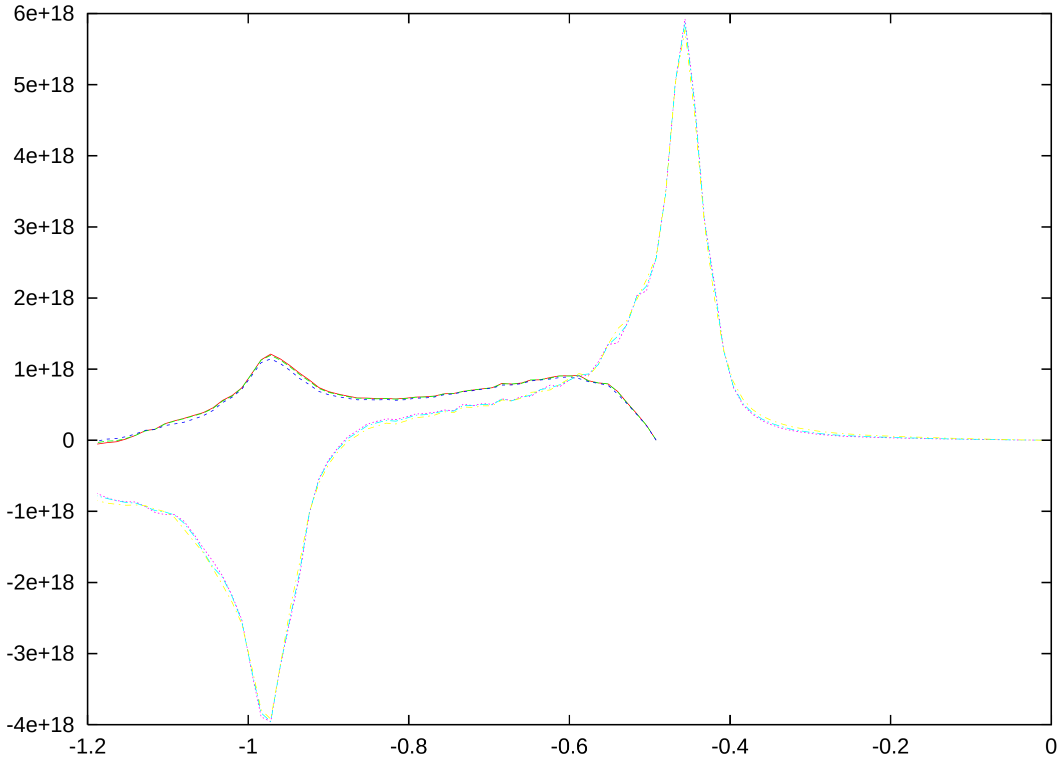

Wake force in V/m/C computed by displacing slice 1 and 40 (out of 100) of a Gaussian bunch (Courtesy G. Rumolo, 2001).

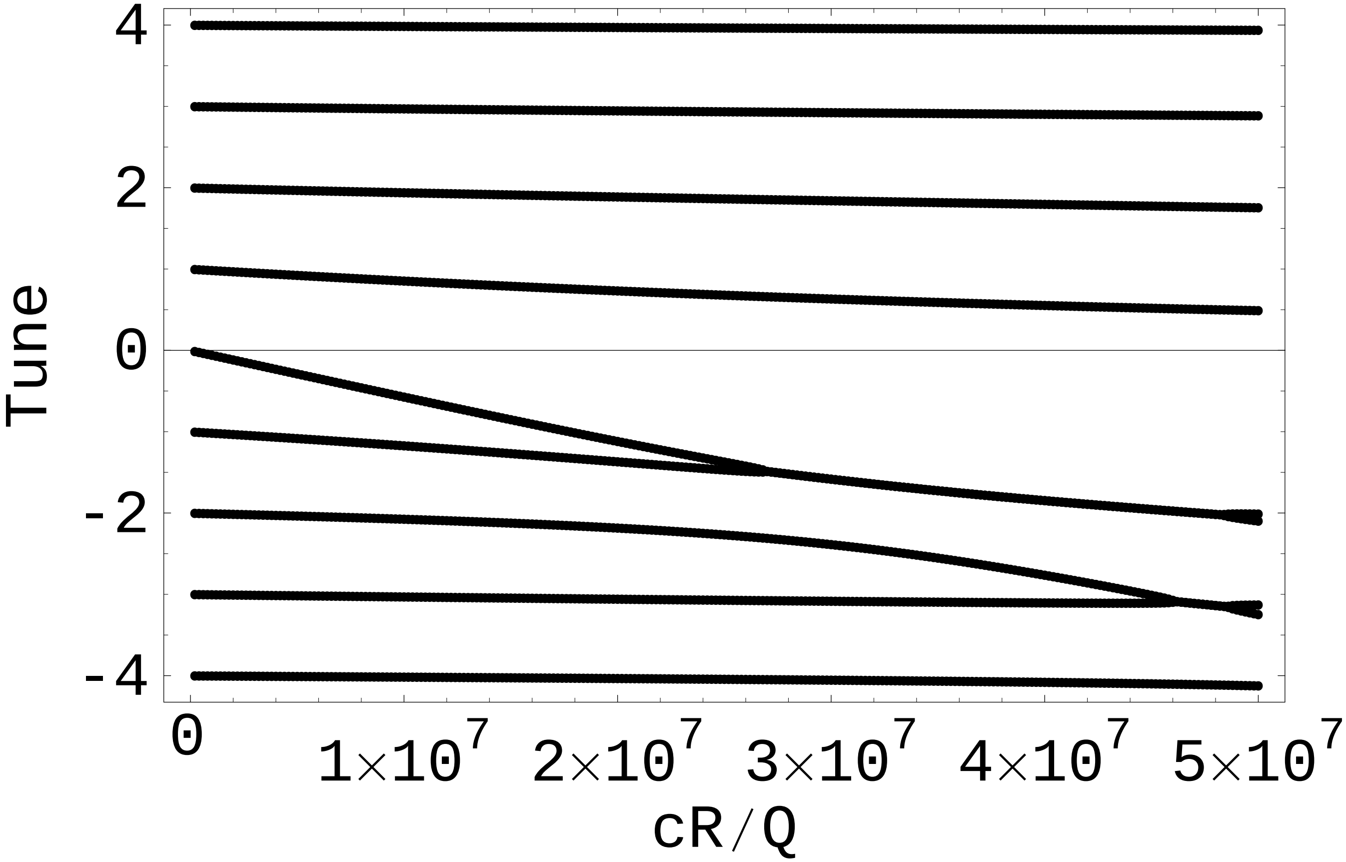

TMCI calculation: betatron side band frequencies $(\omega - \omega_\beta)/\omega_s$ vs. $cR_s/Q \propto \rho_e$ for KEKB LER. [K. Ohmi et al., HEACC'01]. (Courtesy K. Ohmi, 2001).

estimated TMCI thresholds

accelerator	PEP-II	KEKB	PS	SPS	LHC	PSR	SNS
e$^-$ osc./bunch $n_{\rm osc} \equiv \omega_e \sigma_z/(\pi c)$	0.8	1.0	1	0.75	3	34	970
TMCI threshold ρ_e [10^{12} m^{-3}]	1	0.5	5	0.25	3	(0.6)	(0.5)
density ratio $\rho_{e,\rm sat}/\rho_{e,\rm thresh}$	**19**	**4**	0.35	**11**	**4**	(92)	(27)

Detail of the sum (top) and delta (bottom) signals at the SPS provided by the wide-band transverse pick-up in the vertical plane. Head-tail motion inside the bunches is visible. (Courtesy G. Arduini, 2001). Wake period determined from measured head-tail motion: $\lambda_{e^-,\mathrm{wake}} \approx \sigma_z$! (K. Cornelis).

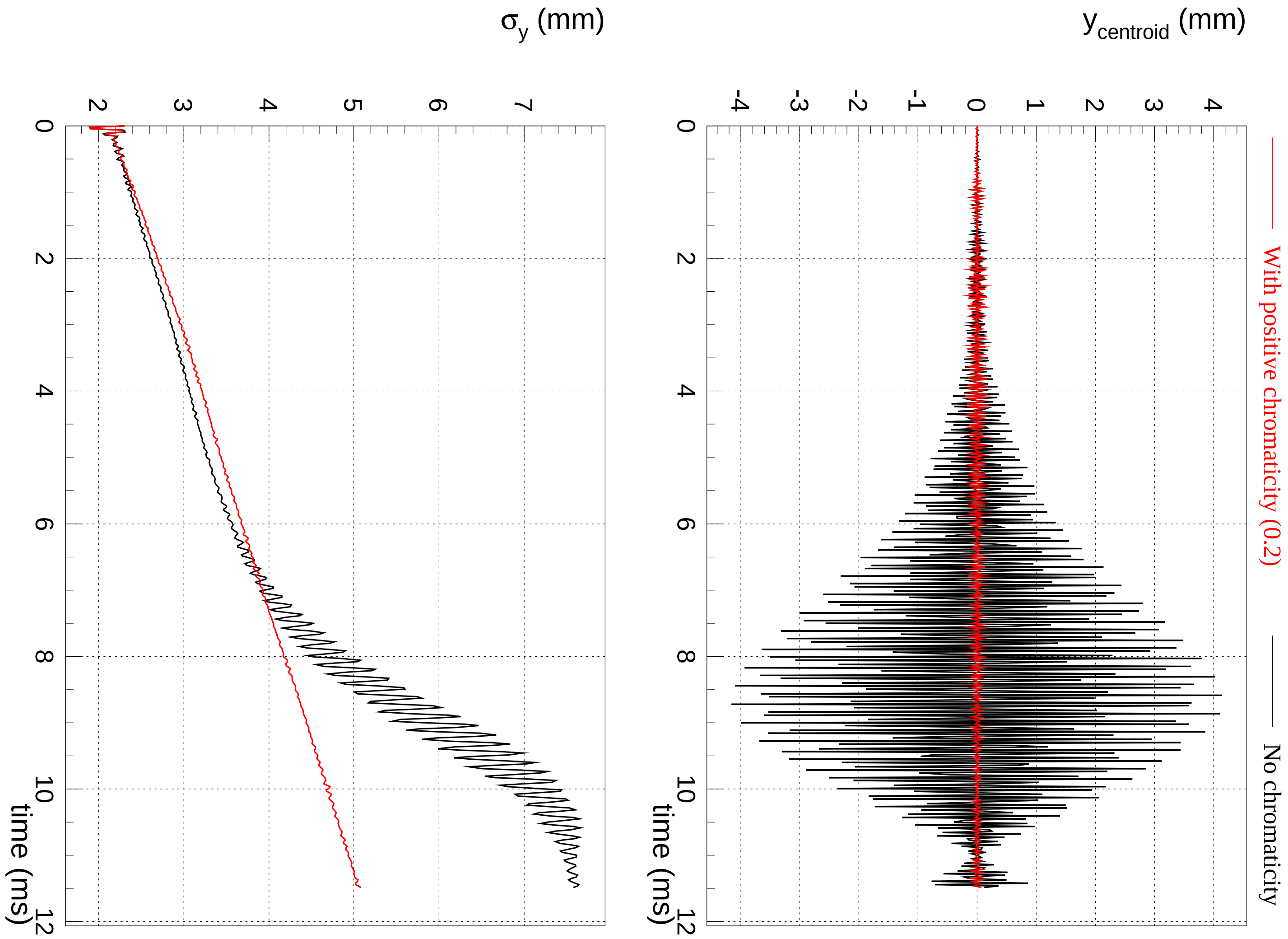

Simulated centroid motion and vertical beam size with zero and positive chromaticity in the SPS ($\xi_y = 0.2$). Machine broadband impedance is also included. (Courtesy G. Rumolo, 2001).

Electron-Cloud Heat Load

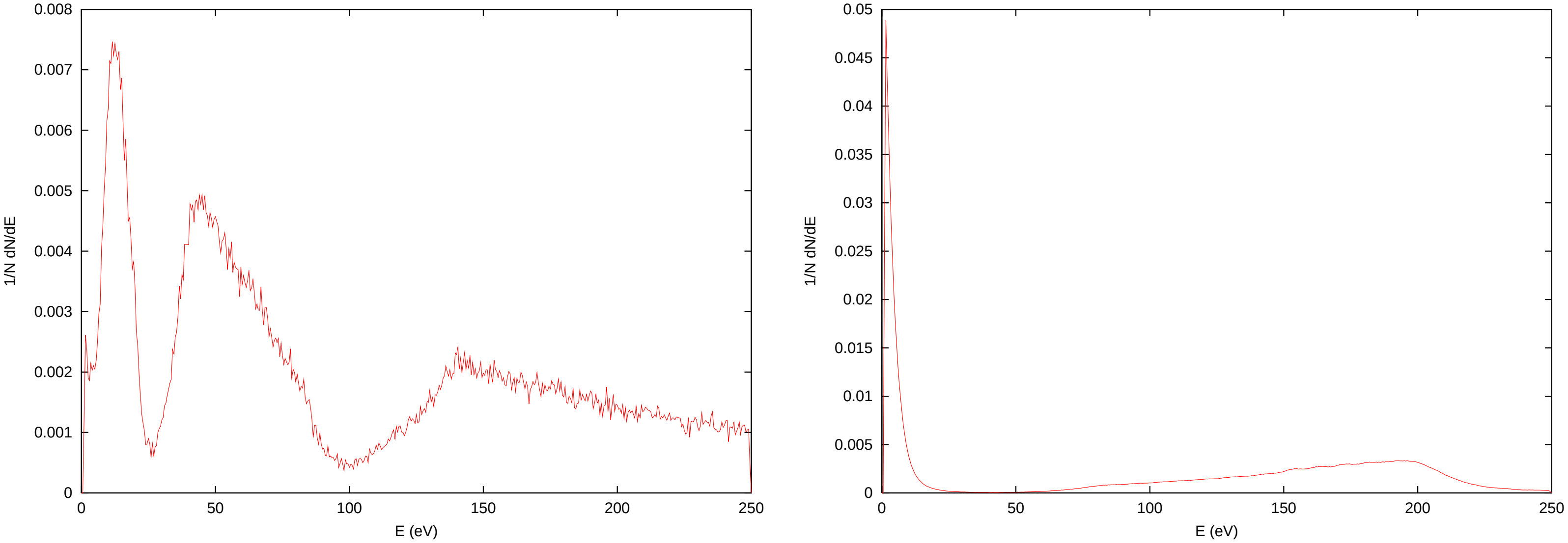

Energy distribution of e^-s incident on LHC chamber wall for a chamber radius $r = 158$ mm (left) and 29 mm (right) (G. Rumolo).

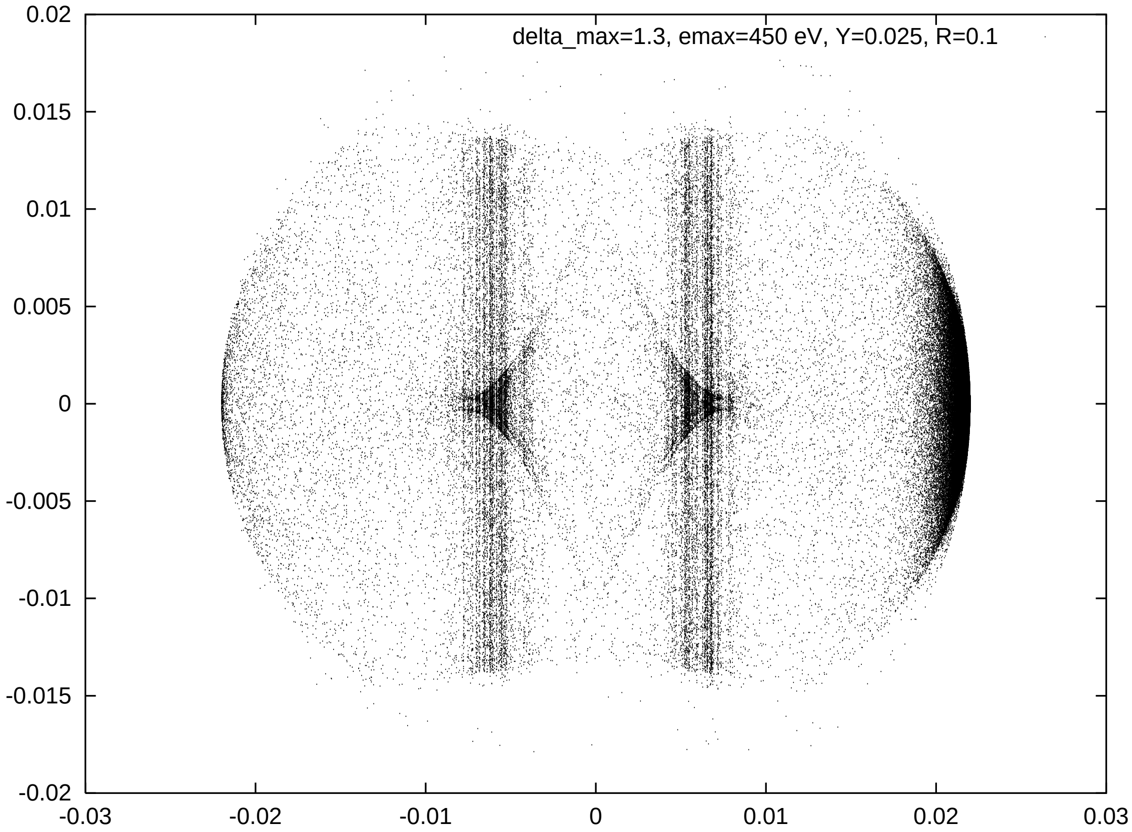

Snapshot of transverse e$^-$ distribution in an LHC dipole chamber (F.Z., 1997). Parameters: $\delta_{\max} = 1.3$, $\epsilon_{\max} = 450$ eV, $R = 0.1$, and $Y^* = 0.025$.

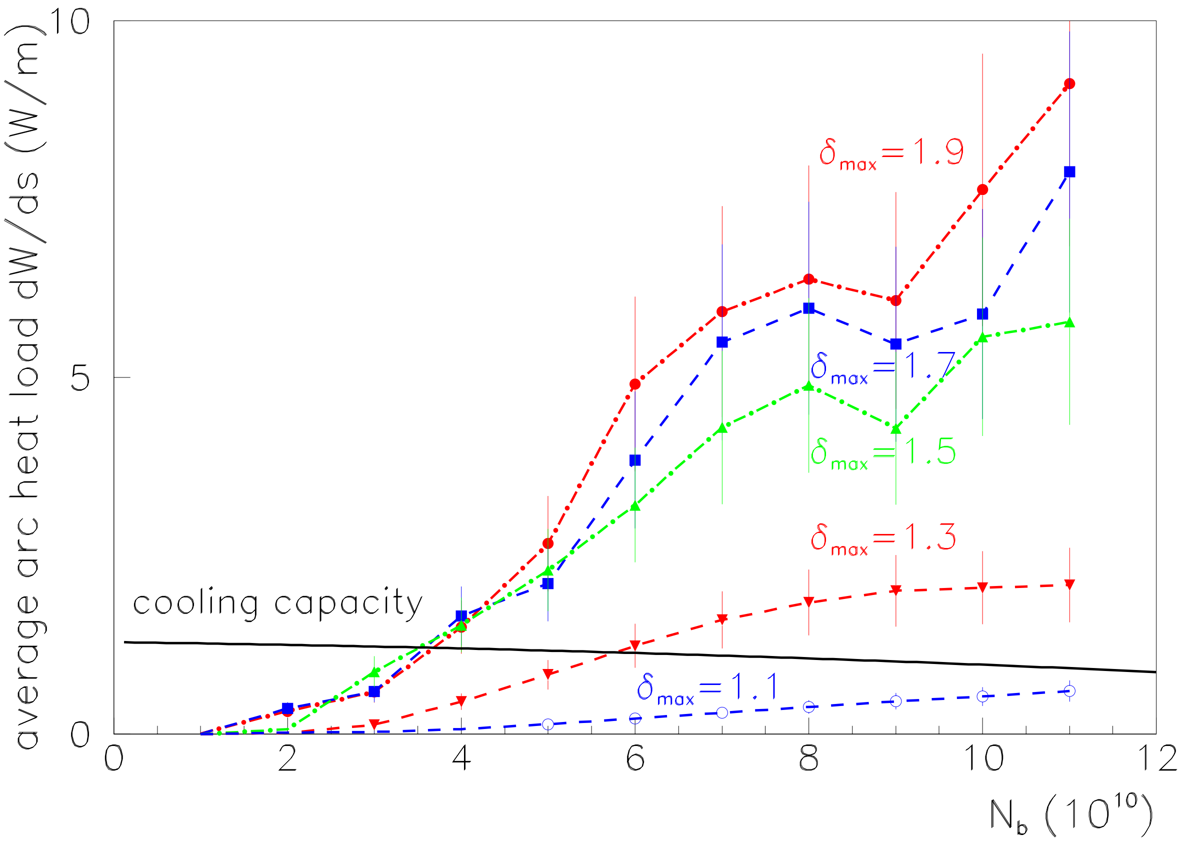

Average arc heat load and cooling capacity as a function of bunch population N_b, for various $\delta_{\rm max}$. Other parameters are $\epsilon_{\rm max} = 240$ eV, $R = 5\%$, $Y = 5\%$, and elastic electron reflection is included.

LHC Recipe

- in arc dipoles: use sawtooth chamber to reduce photon reflections
- coat all warm sections with getter material TiZr (low secondary emission yield)
- rely on surface scrubbing during the commissioning to reduce the maximum secondary emission yield to a value of 1.1

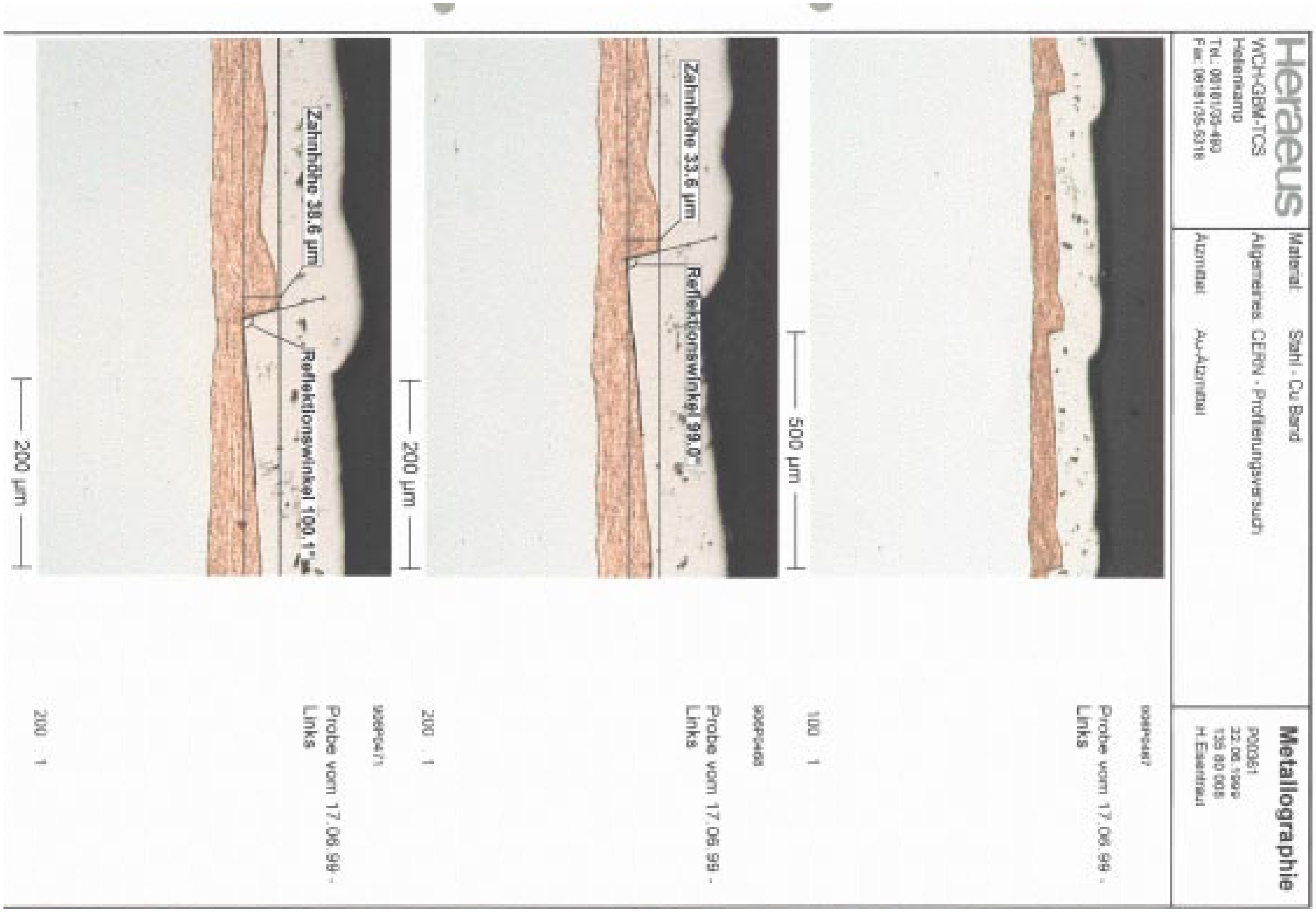

Sawtooth chamber protoype; the sawtooth reduces the photon reflectivity R to 1.3% [co-laminated Cu: $R \approx 80\%$]. (Ian Collins).

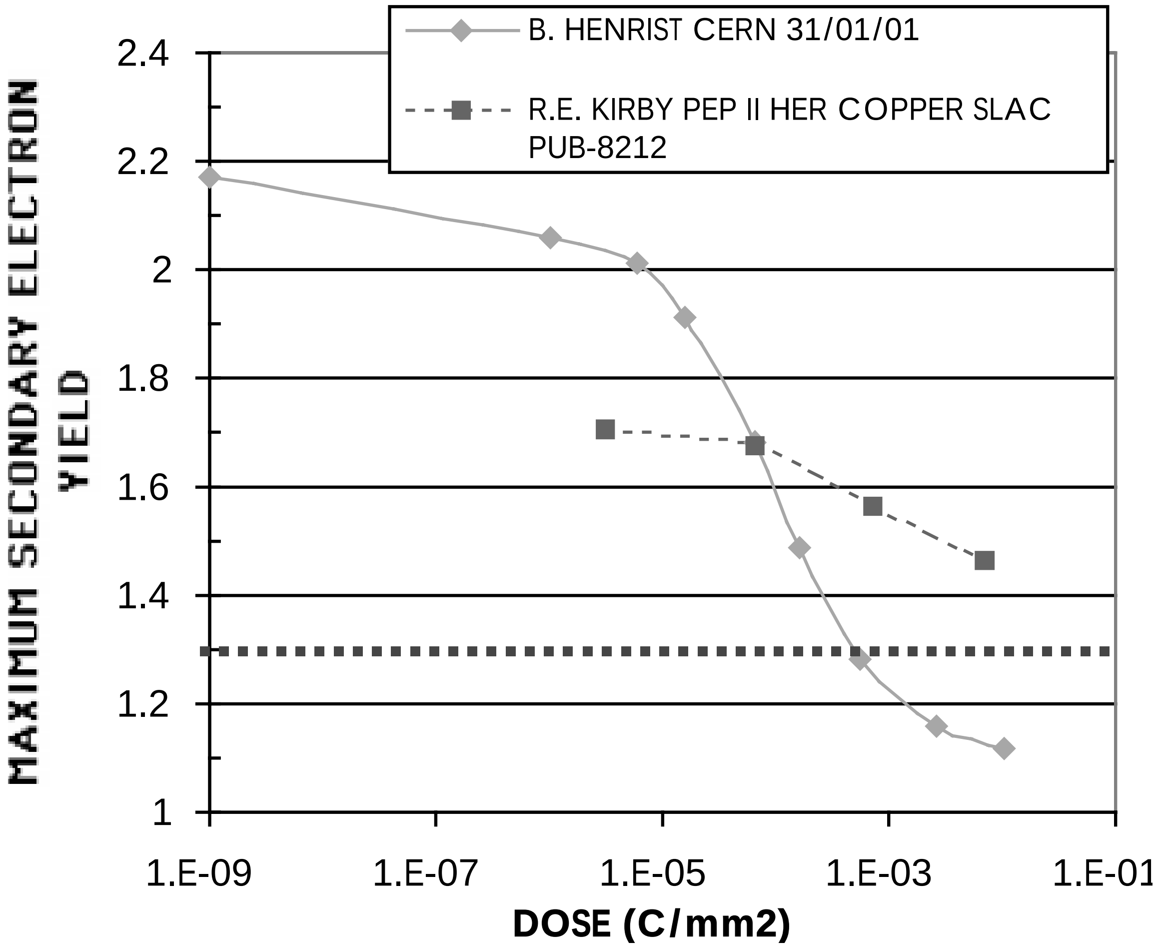

Comparison of dose dependence of the Secondary Emission Yield as maeasured at CERN and SLAC (N. Hilleret et al., 2001).

Newly Installed SPS e^- Cloud Detectors

- Pick-ups for e^- characteristics
  - e^- cloud build up, e^- energy distribution, triggering on the batch
- Behavior of e^- in a dipole magnetic field
  - ‘strip detector’
  - ‘triangle detector’
- Scrubbing effect by in-situ measurement of secondary emission yield
- Ion detectors to exclude ion-stimulated desorption
- WAM_PAC Cu calorimeter to directly measure heat load from e^{-1} cloud

Cu Calorimeter

WAMPAC in BA4

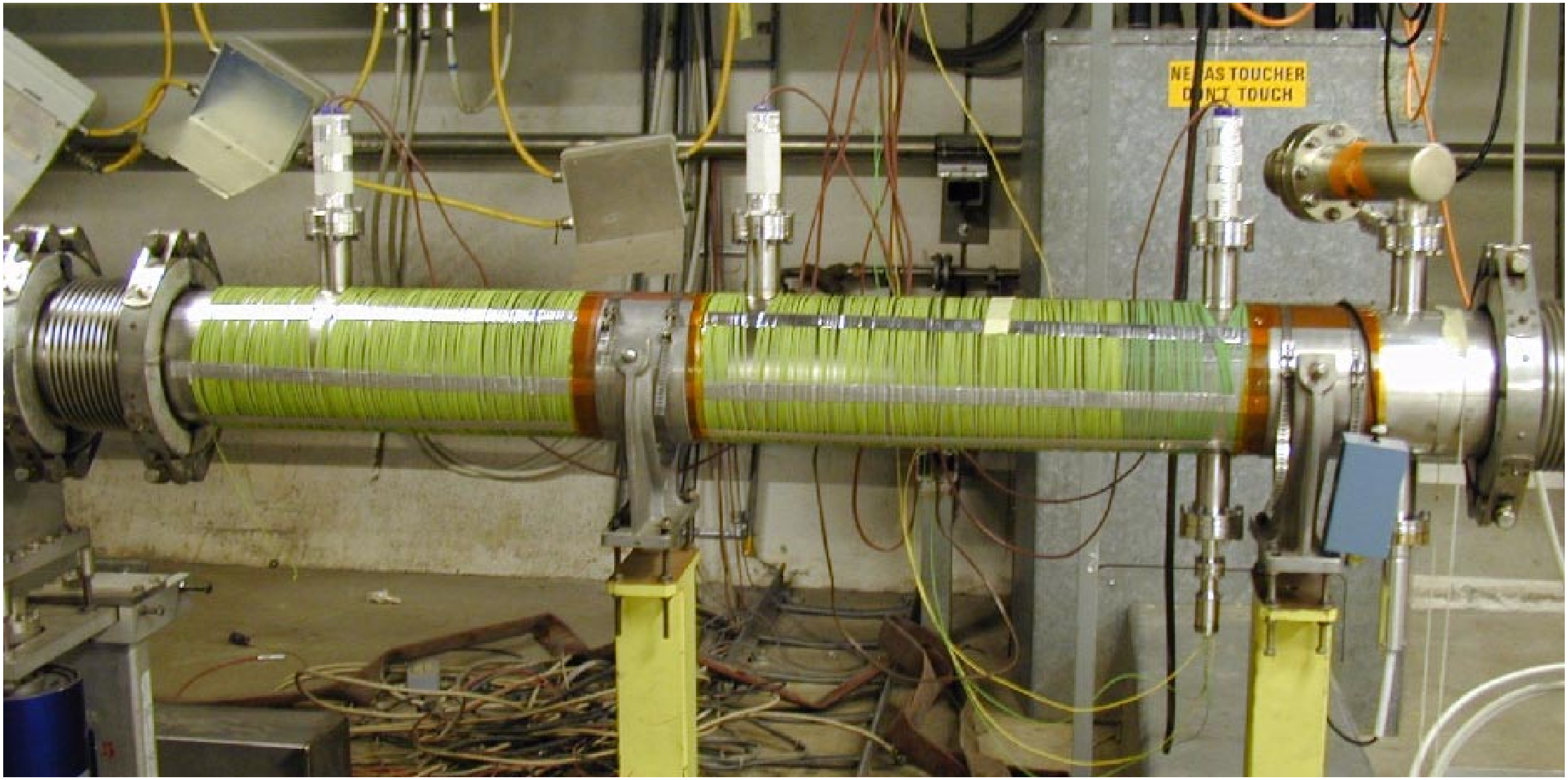

#1 Calibration : Q = 5 W

$$\frac{\Delta T}{\Delta t} = \frac{\dot{Q}}{m\,C_p} = 0.25\,\mathrm{K/min}$$

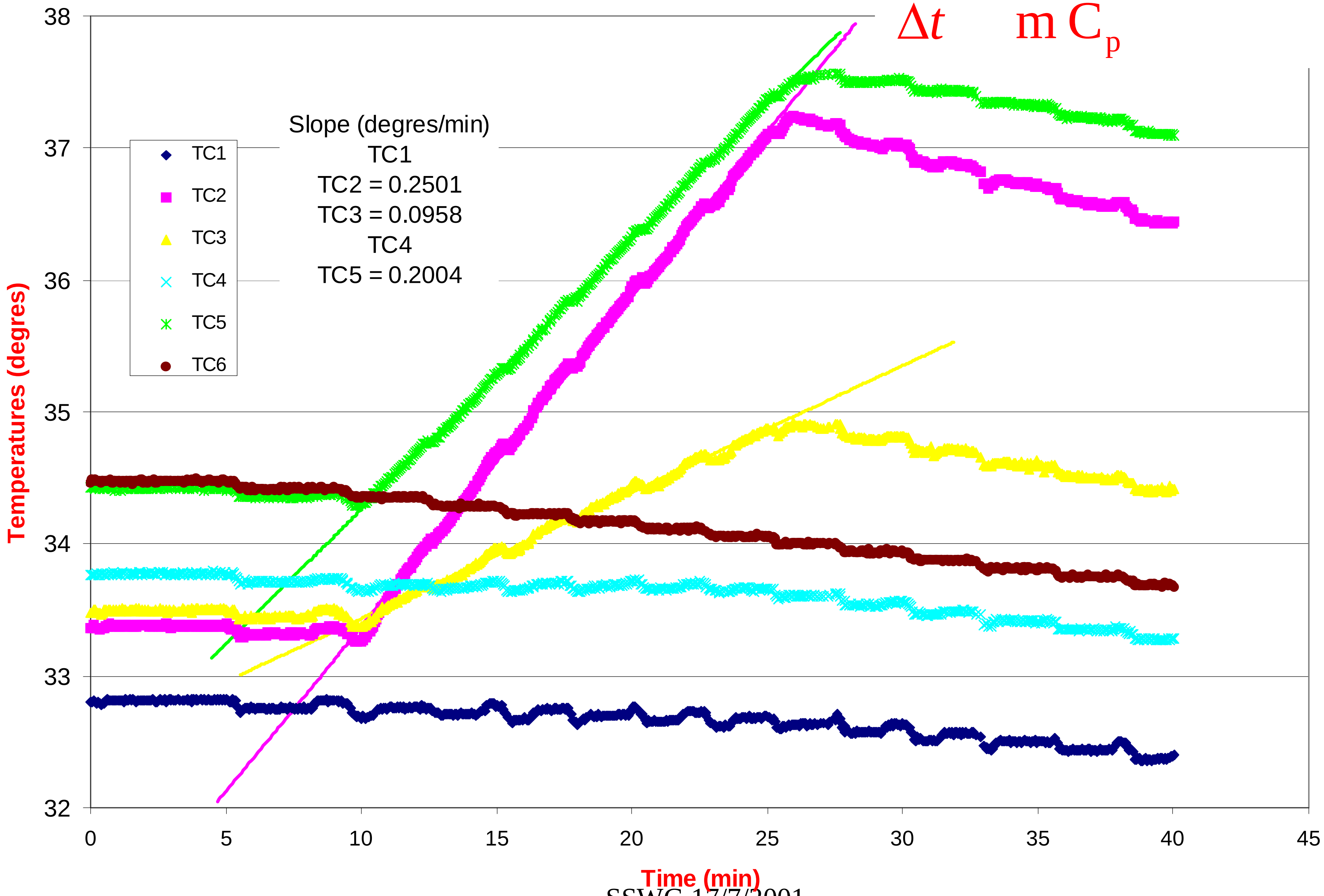

Triangle detector

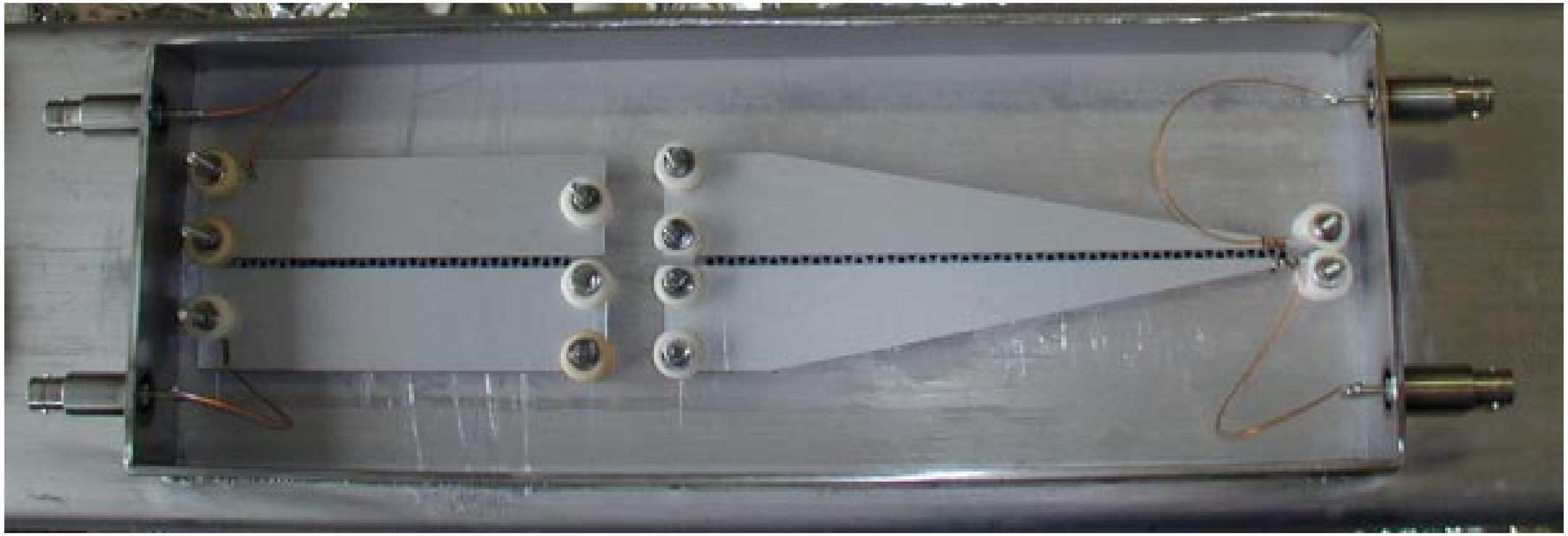

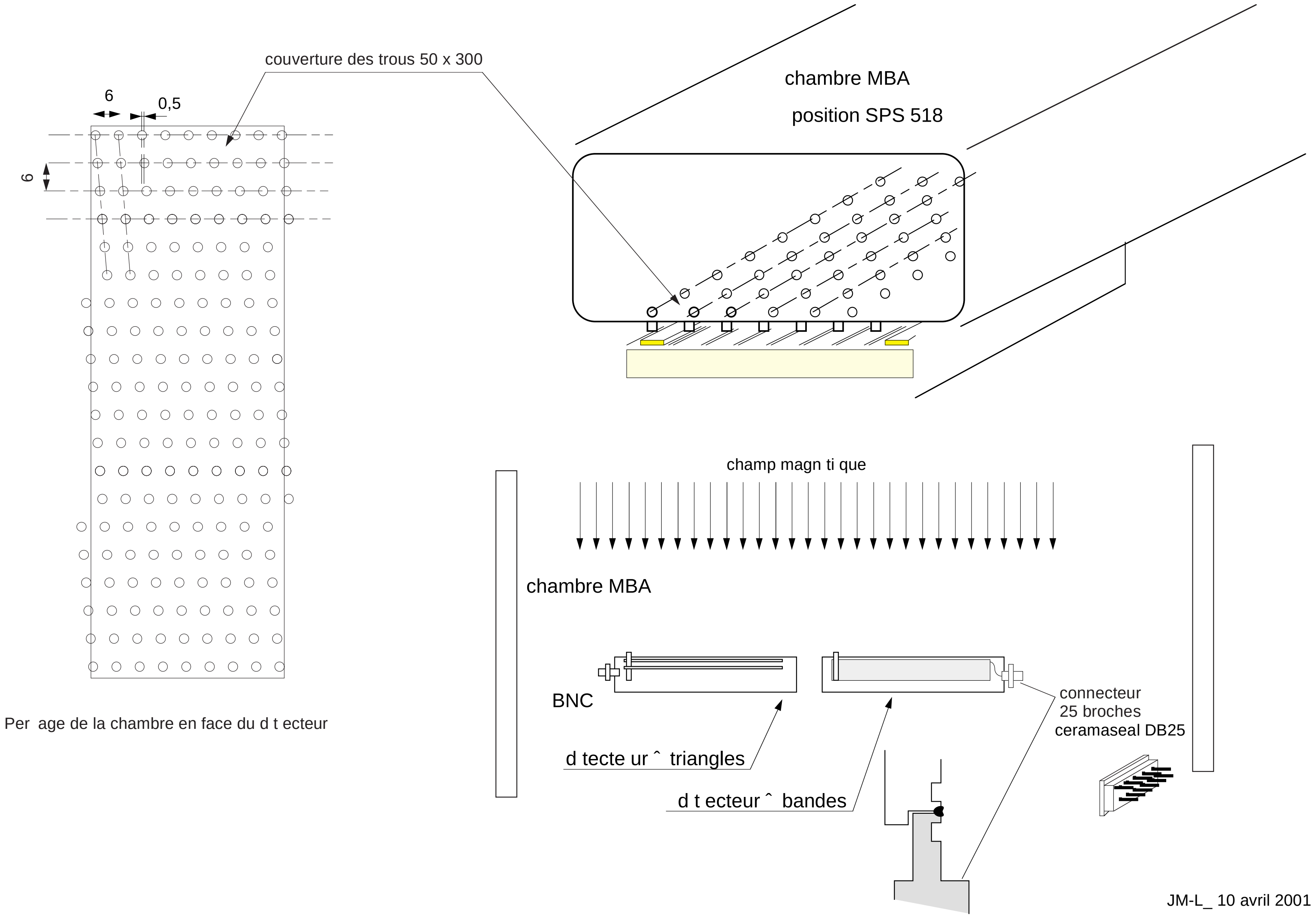
couverture des trous 50 x 300
6
0,5
6
chambre MBA
position SPS 518
Perçage de la chambre en face du détecteur
champ magnétique
chambre MBA
BNC
connecteur
25 broches
ceramaseal DB25
détecteur à triangles
détecteur à bandes
JM-L_ 10 avril 2001

Strip detector

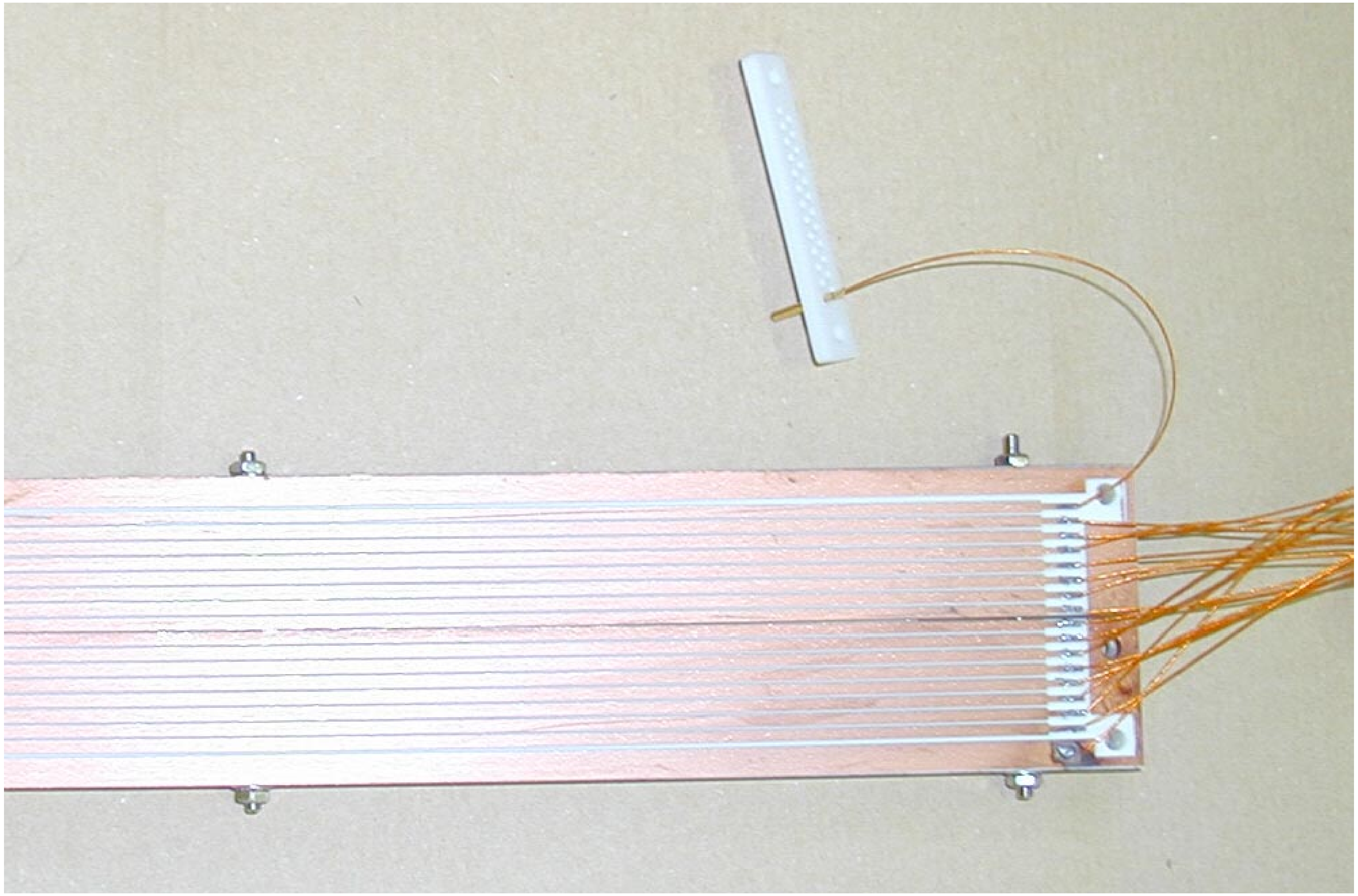

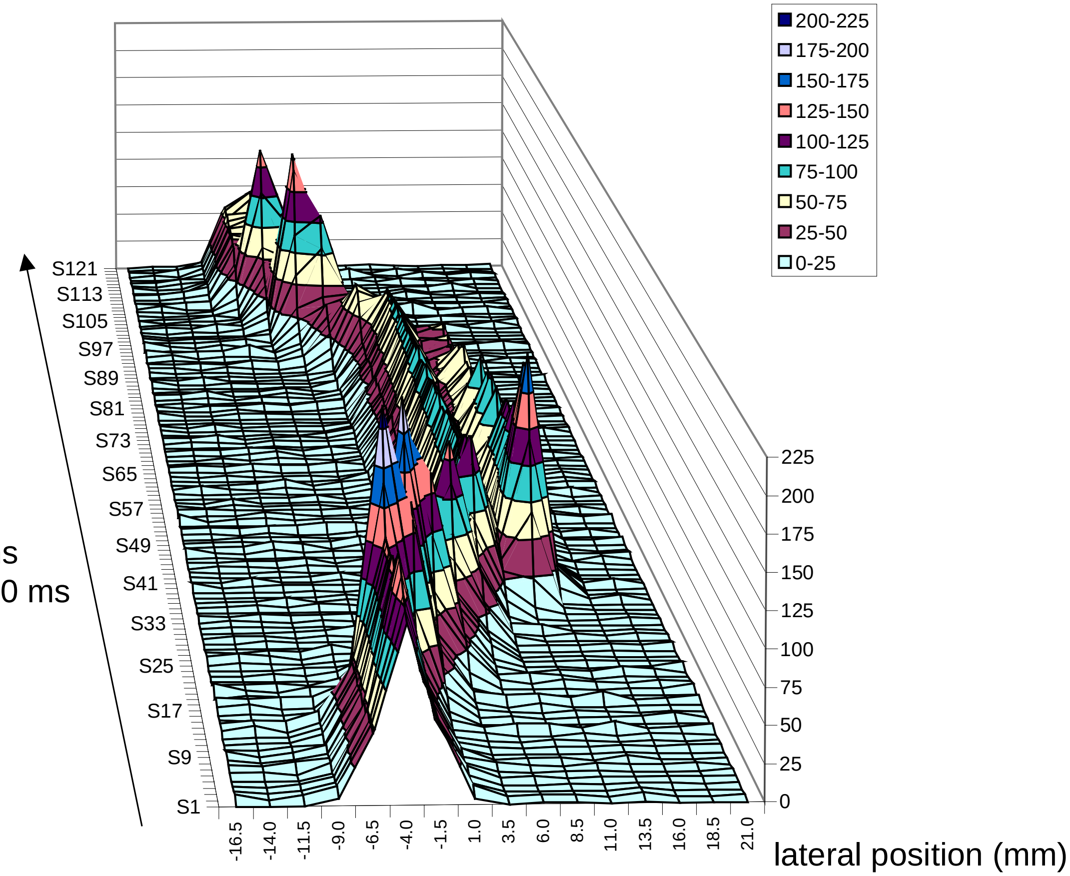

Integration: 20 ms
Sampling time: 20 ms

Stripe signal for 8.5 mm orbit bump with 2 s duration. The stripe clearly follows the beam. (G. Arduini, et al., 2001).

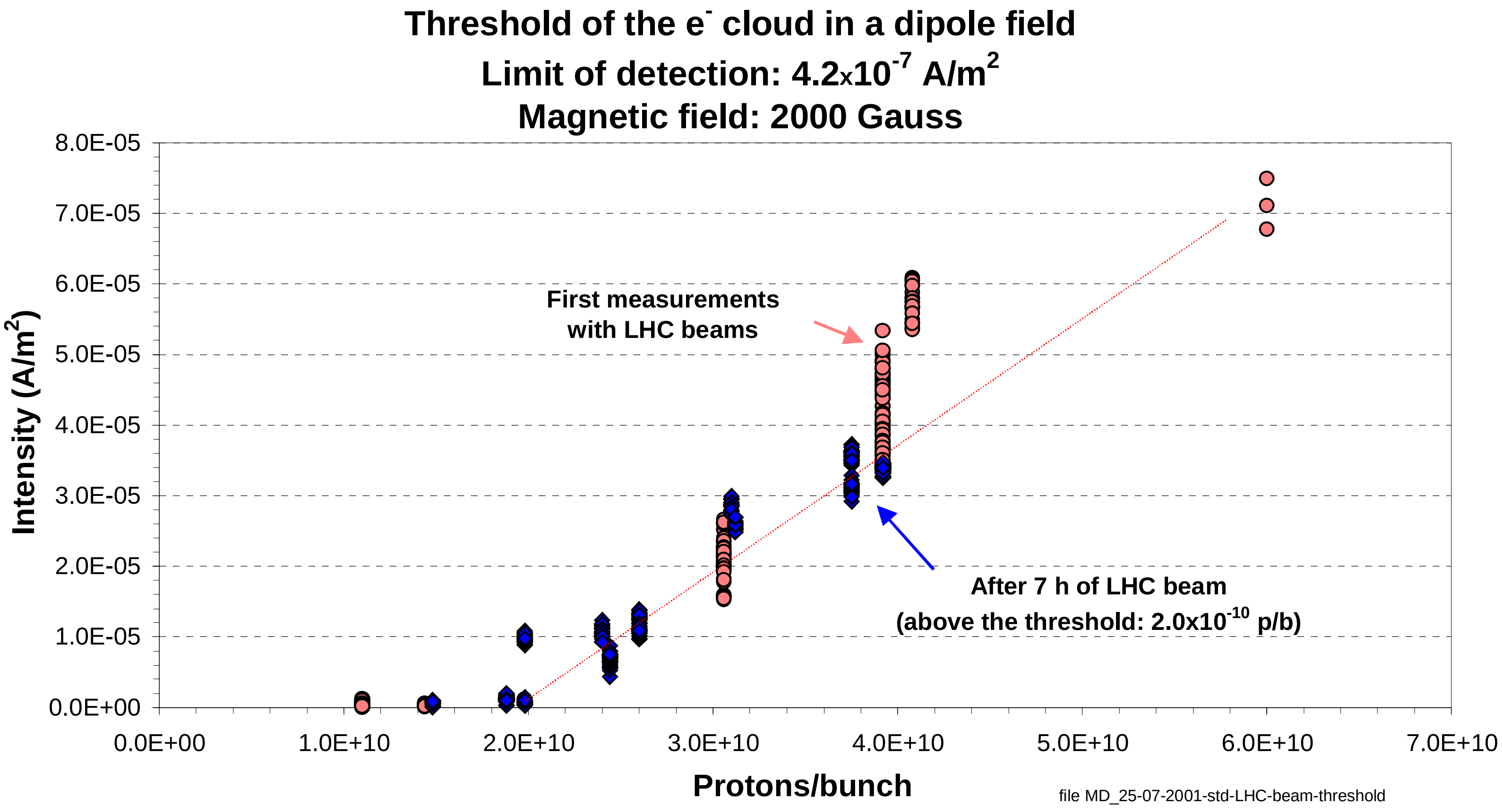

Threshold of the e^- cloud in a dipole field

Limit of detection: 4.2×10^{-7} A/m^2

Magnetic field: 2000 Gauss

First measurements with LHC beams

After 7 h of LHC beam (above the threshold: 2.0×10^{-10} p/b)

file MD_25-07-2001-std-LHC-beam-threshold

Electron-stripe intensity in a 2-T dipole field vs. bunch population. Threshold at 2×10^{10} protons per bunch.

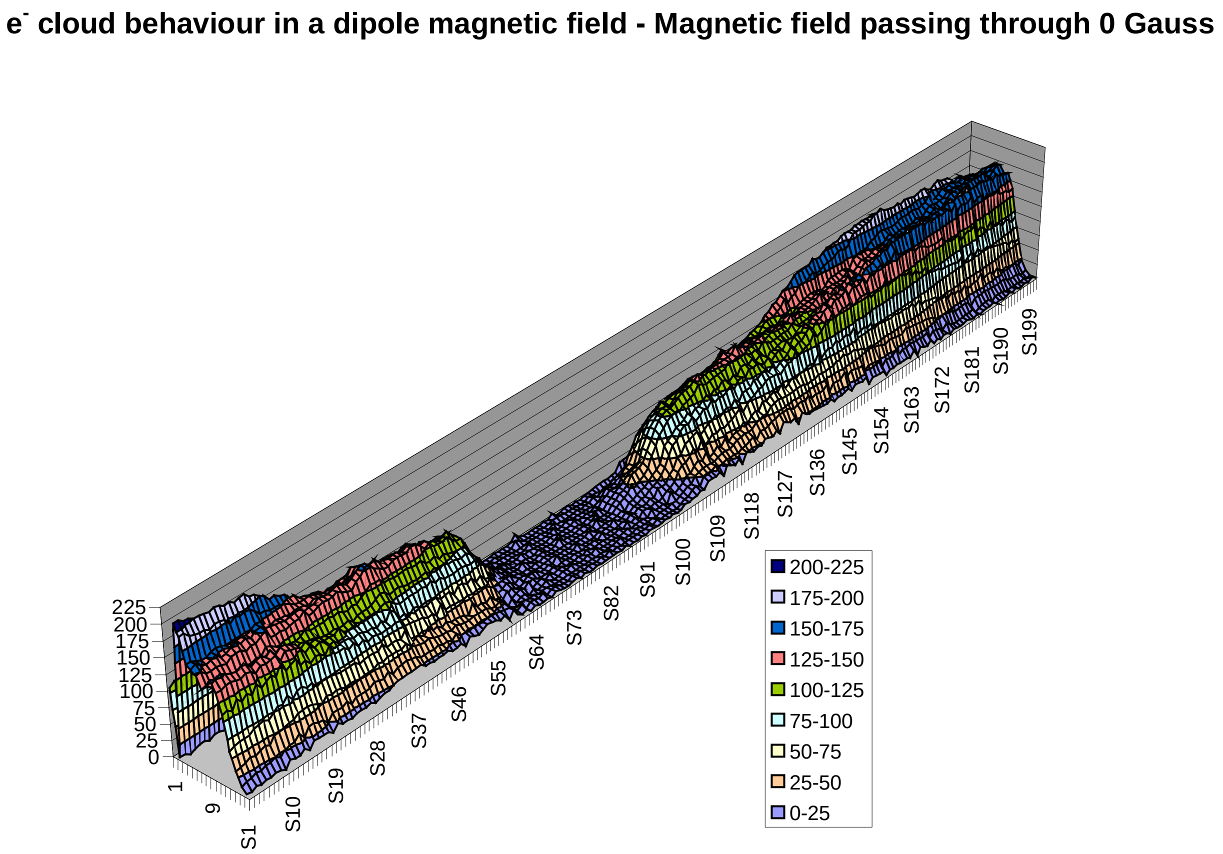

e$^-$ stripe vs. magnetic field; signal disappears for $|B| \leq 15$ G.

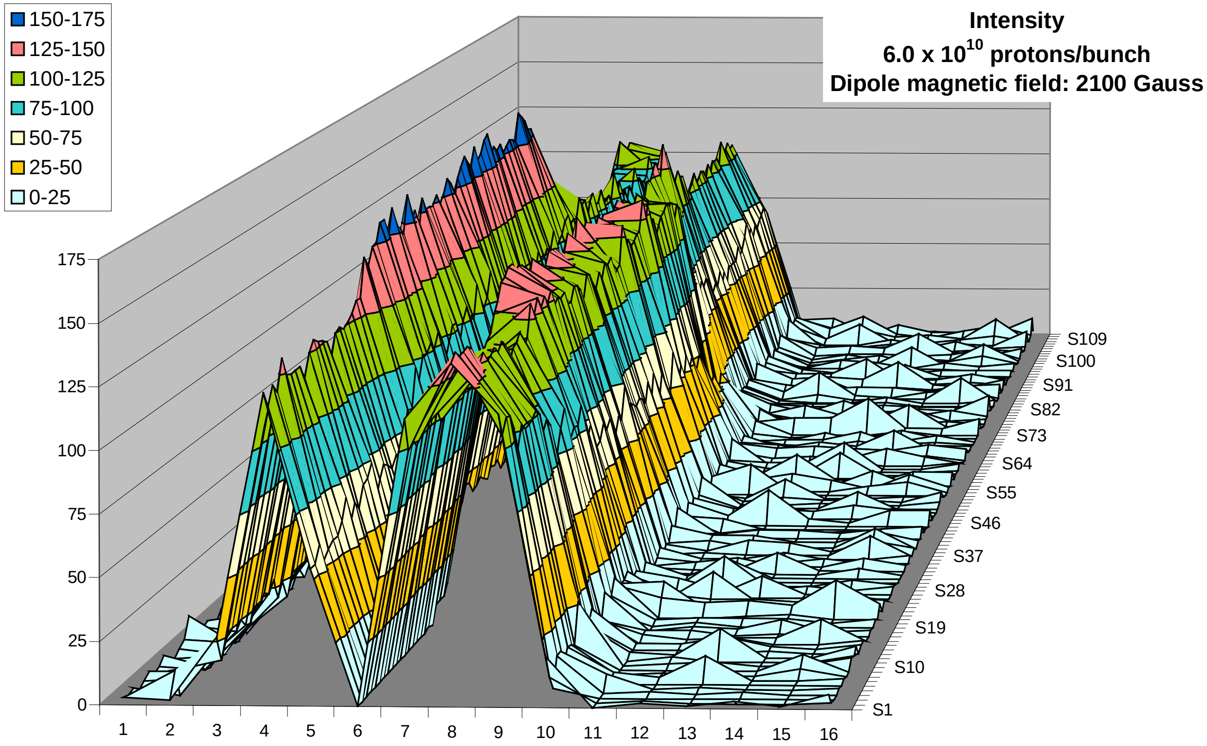

At higher intensity $N_b \approx 6 \times 10^{10}$ two stripes are observed! Spacing consistent with simulation.

(C) Beyond LHC: LHC-II and VLHC

- higher luminosity and/or energy
- more bunches?
- crossing angle & crabbing
- magnets (stronger and/or cheaper)
- synchrotron radiation
- emittance control
- collective effects & electron cloud
- IP debris, quench limits, & safe beam abort
- quasi-continuous beams?

Luminosity for Bunched Beams

$$L = \frac{N_b^2 f_{\rm rep} H_D}{4\pi\sigma_x\sigma_y}\ \eta_L$$

For a horizontal crossing, η_L is

$$\eta_L = \frac{2}{\sigma_z\sqrt{\pi}} \int_0^\infty \frac{\exp\left(-\left(\frac{z}{\sigma_z}\right)^2 \left\{1+\frac{\theta_c^2}{4\theta_d^2}\left[\frac{1}{1+(z/\beta_x^*)^2}\right]^2\right\}\right)}{\sqrt{(1+(z/\beta_x^*)^2)\ (1+(z/\beta_y^*)^2)}}$$

where $\theta_d = \sigma_x/\sigma_z$, θ_c the full crossing angle.

Beam-Beam Tune Shifts for Bunched Beams

Assuming $\beta_x^* \approx \beta_y^*$ and $\epsilon_x \approx \epsilon_y$ the beam-beam tune shifts for a particle at the center of the bunch are

$$\begin{aligned}
\Delta Q_x \quad &= \quad -\frac{N_b r_p}{2\pi\gamma}\frac{1}{\sqrt{2\pi}\sigma_z}\int_{\infty}^{\infty}\left(\beta^* + \frac{s^2}{\beta^*}\right)\left[\left(\frac{1}{\left(\beta^* + s^2/\beta^*\right)\epsilon} + \frac{1}{\theta_c^2 s^2}\right)\right. \\
&\qquad \left.\exp\left(-\frac{\theta_c^2 s^2}{2\left(\beta^* + s^2/\beta^*\right)\epsilon}\right) - \frac{1}{\theta_c^2 s^2}\right]\exp\left(-\frac{s^2}{2\sigma_z^2}\right)\ ds \\
\Delta Q_y \quad &= \quad -\frac{N_b r_p}{2\pi\gamma}\frac{1}{\sqrt{2\pi}\sigma_z}\int_{\infty}^{\infty}\left(\beta^* + \frac{s^2}{\beta^*}\right)\left[\frac{1}{\theta_c^2 s^2}\left(1 - \right.\right. \\
&\qquad \left.\left.\exp\left(-\frac{\theta_c^2 s^2}{2\left(\beta^* + s^2/\beta^*\right)\epsilon}\right)\right)\right]\exp\left(-\frac{s^2}{2\sigma_z^2}\right)\ ds\ ,
\end{aligned}$$

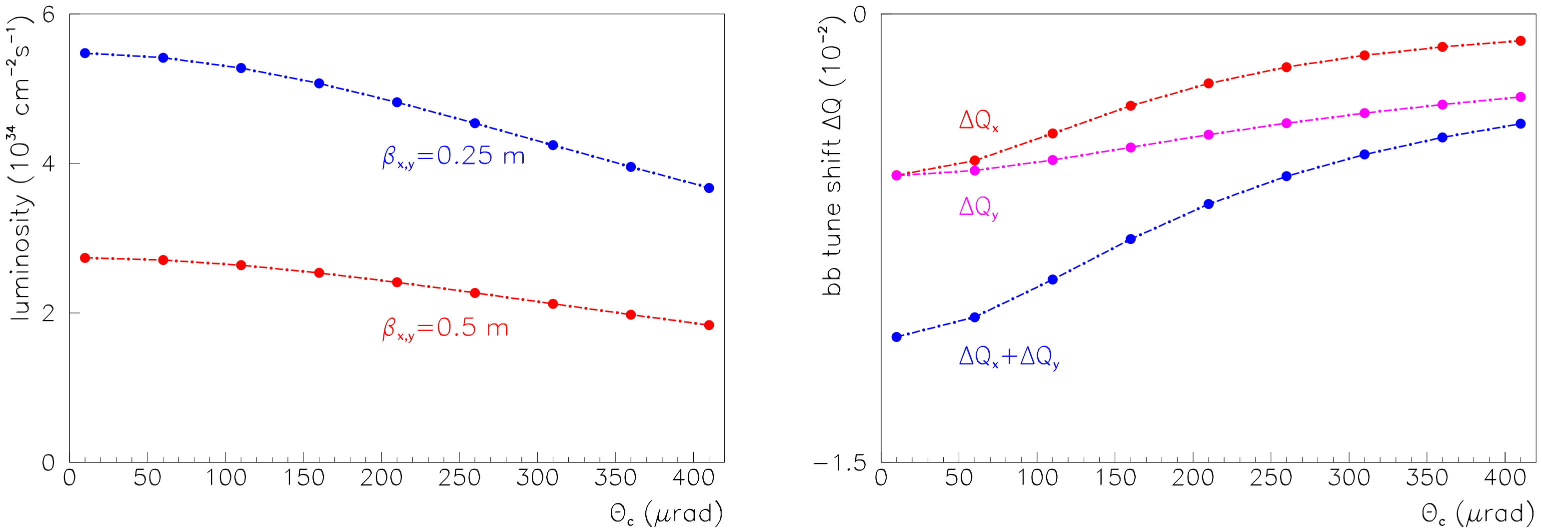

Luminosity (left) and total beam-beam tune shift (right) vs. crossing angle; parameters: $N_b = 1.7 \times 10^{11}$, $\beta^* = 0.25$ m, $\sigma_z = 7.7$ cm, $n_b = 2800$, $\gamma\epsilon_\perp = 3.75$ μm.

Crab Cavities

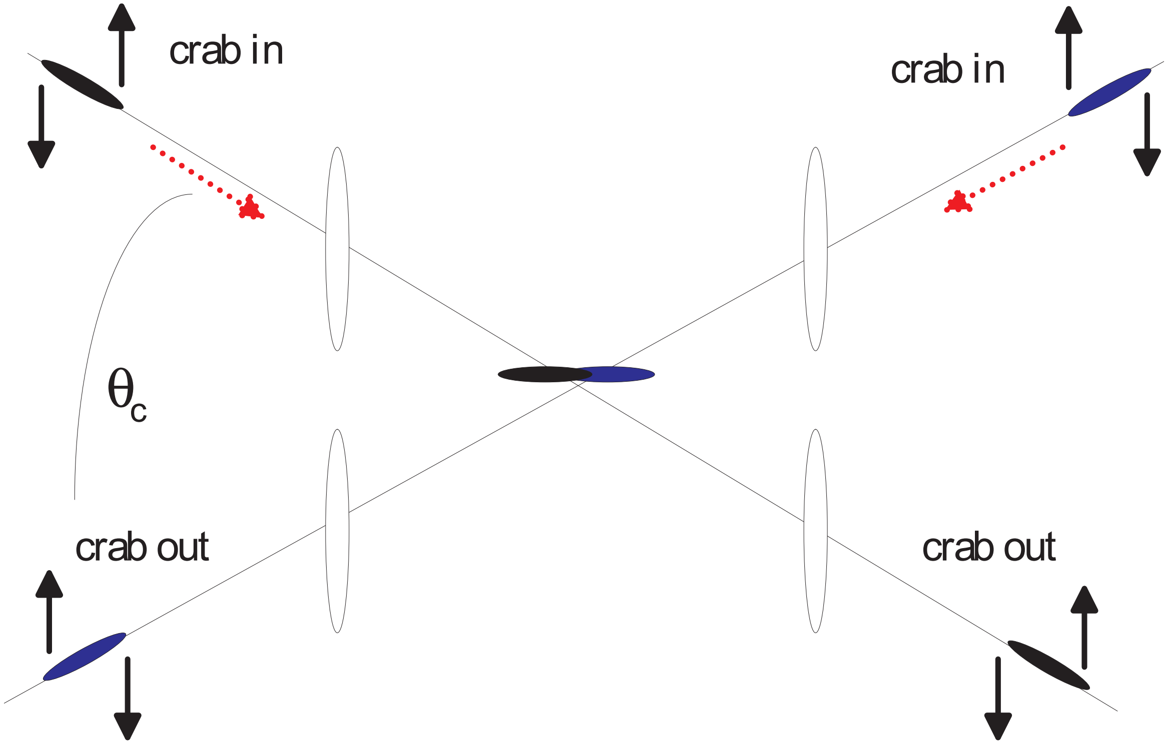

Applying a deflection of opposite sign to the head and tail of each bunch, luminosity loiss due to the crossing angle is avoided.

Crab Cavities cont'd

Distance between last quadrupole and IP about 20 m. Outer quadrupole radius 25 cm. Two separate final quadrupoles require $\theta_c \geq 25$ mrad. Transverse crab deflecting voltage:

$$V_\perp = \frac{cE \tan\theta_x/2}{e\omega_{rf}\sqrt{\beta_x^*\beta_{\rm crab}}}$$

variable	symbol	KEKB HER	LHC
beam energy	E	8.0 GeV	7 TeV
RF frequency	$f_{\rm rf}$	508.9 MHz	1.3 GHz
half crossing angle	$\theta_c/2$	11 mrad	12.5 mrad
IP beta function	β_x^*	0.33 m	0.25 m
cavity beta function	β_x	100 m	2000 m
required kick voltage	$V_\perp$	1.44 MV	144 MV

phase diagram ofNb$_3$Sn

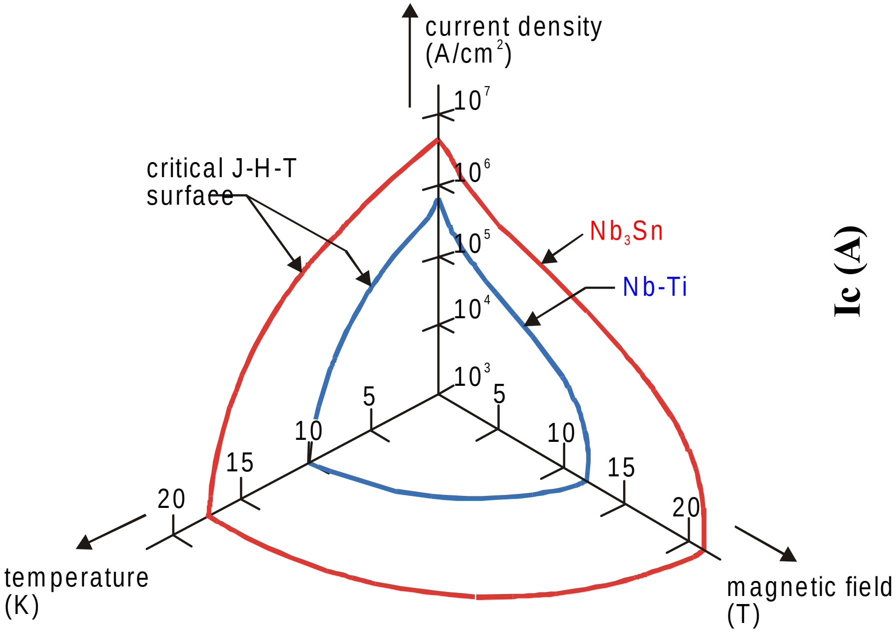

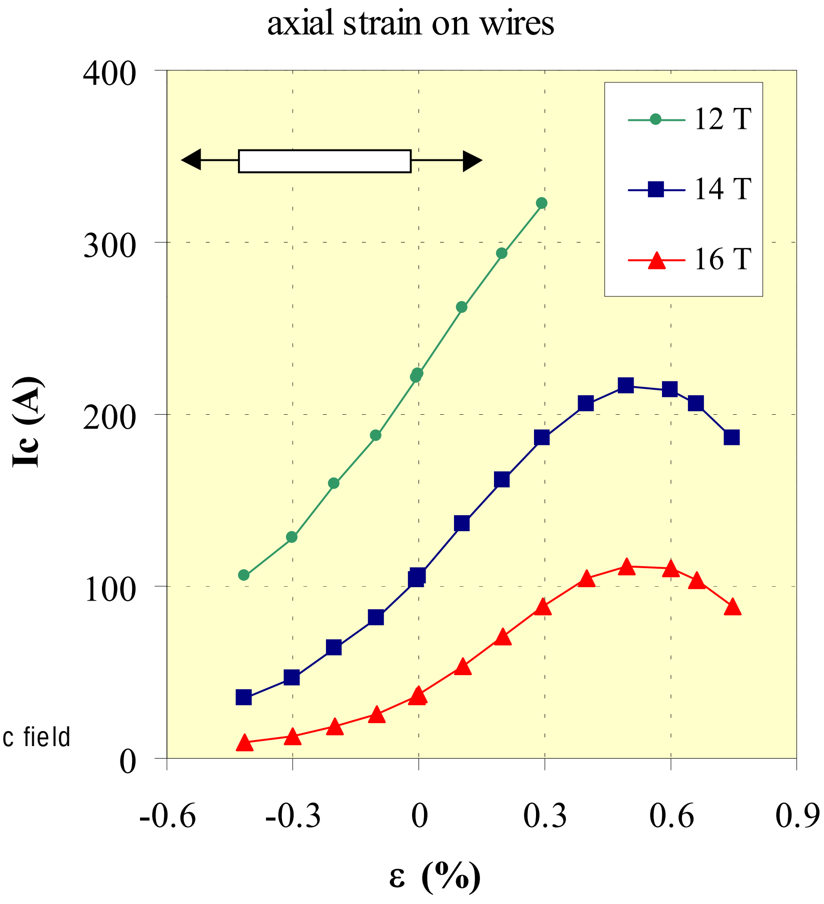
axial strain on wires

ε= 0 after cool-down to 4.2 K

Stronger Magnets? Nb_3Sn instead of $NbTi$

year	group	type	field/gradient
1982	CERN	quad	71 T/m
1983	CERN/Saclay	dipole	5.3 T
1985	LBL	dipole D10	8 T
1986	KEK	dipole	4.5 T
1988	BNL	dipole	7.6 T
1991	CERN-ELIN	dipole	9.5 T
1995	LBNL	hybrid dipole D19H	8.5 T
1995	UT-CERN	dipole MSUT	11.2 T
1996	LBNL	dipole D20	13.3 T
2001	LBNL	common coil dipole	14.4 T

LHC-II Parameters

parameter	LHC	LHC-II
beam energy E [TeV]	7	14
dipole field B [T]	8.39	16.8
total energy/beam [MJ]	334	1130
number of bunches n_b	2800	5600
bunch population N_b [10^{11}]	1.05	1.05
rms IP beam size $\sigma^*_{x,y}$ [μm]	15.9	7.4
rms IP div. $\sigma^*_{x',y'}$ [μrad]	31.7	34
IP beta $\beta^*_{x,y}$ [m]	0.5	0.22
beam-beam tune shift / IP $\xi_{x,y}$	0.0034	0.005
crossing angle θ_c [μrad]	300	300
rms bunch length σ_z [cm]	7.7	4.0

LHC-II Parameters (cont'd)

bunch spacing $L_{\rm sep}$ [m]	7.48	3.74
SR power $P_{\rm SR}$ [kW]	3.6	114
SR dipole heat load dP/ds [W/m]	0.2	6.6
rms transv. emittance $\gamma\epsilon_{x,y}$ [μm]	3.75	3.75 → 1.0
eq. horiz. emittance $\gamma\epsilon_x^{eq}$ [μm]	$2.03^\star$	$1.07^\star$
longit. emittance ϵ_L (σ) [eVs]	0.2	$0.15^\star$
damp. time $\tau_{x,\rm SR}$ [hr]	52	6.5
IBS growth time $\tau_{x,\rm IBS}$ [hr]	142	345 (in.)
events per crossing	18	90
peak luminosity L [10^{34} cm^{-2}s^{-1}]	1.0	10.
lum. lifetime τ [hr]	10	3.2

Emittance Evolution

synchrotron radiation amplitude damping time

$$\tau_z J_z = \left(\frac{3(m_p c^2)^3}{e^2 c^3 r_p Z^2}\right) \frac{1}{B^2 E} \left(\frac{C}{2\pi\rho}\right) \approx \frac{16644\mathrm{hr}}{E[\mathrm{TeV}]B[\mathrm{T}]^2} \left(\frac{C}{2\pi\rho}\right) \frac{A^4}{Z^4}$$

damping decrement (for 2 IPs)

$$\delta = \frac{T_0}{n_{\mathrm{IP}}\tau_{x,y}} \approx 5.7 \times 10^{-13}\ E[\mathrm{TeV}]^2 B[\mathrm{T}] \frac{Z^3}{A^4}$$

does this affect the maximum beam-beam tune shift?

maximum ξ: measurements and simulations fitted by

$$\xi_{\max} \propto 0.009 + 0.021\ (\delta/10^{-4})^{0.5}$$

[E. Keil & R. Talman, 1983; S. Peggs, 1999; R. Assmann et al., 2000]

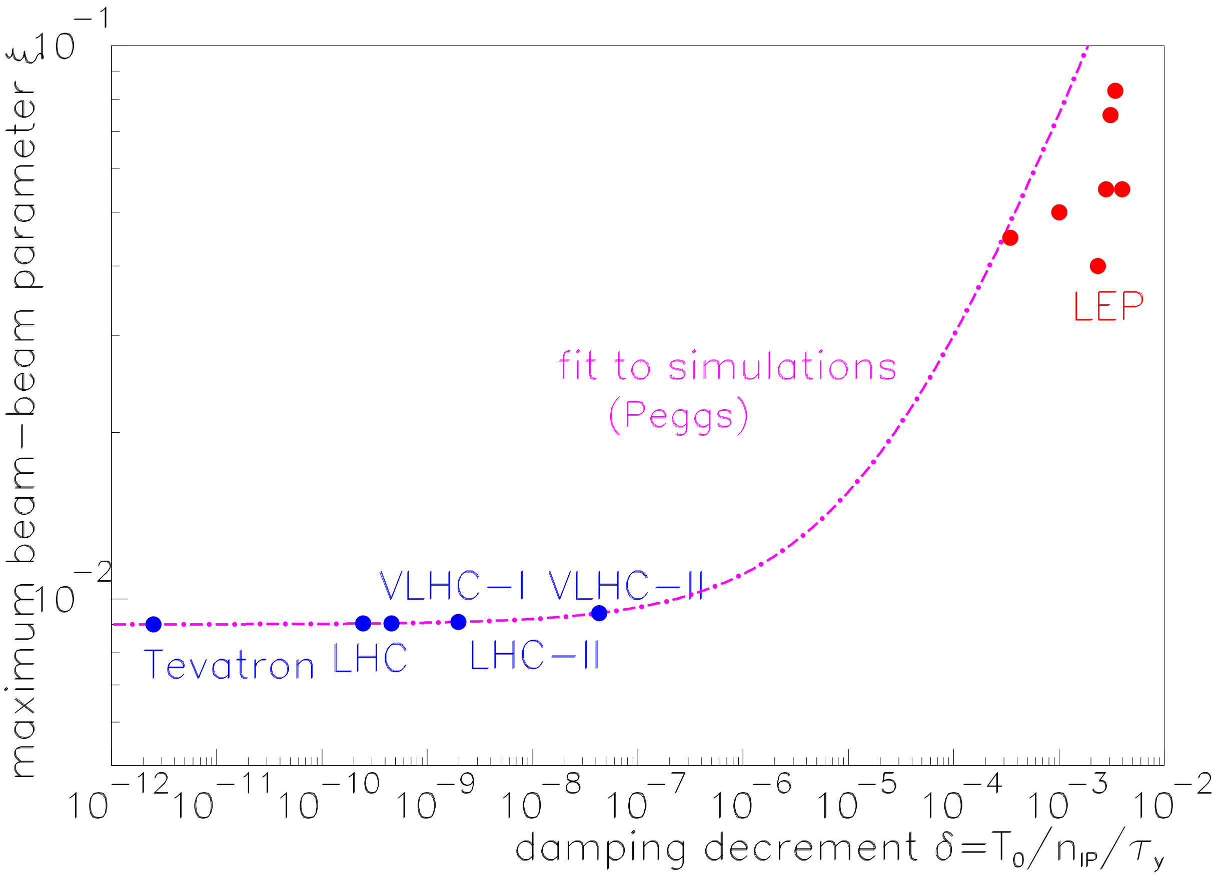

Tune shift parameter vs. damping decrement. [LEP data courtesy of R. Assmann; not beam-beam limited]

more important consequence of synchrotron radiation: **shrinkage of emittance during the store**

situation different from e$^-$ storage rings; $\tau_{\rm SR}$ ~hours

SR equilibrium emittance:

$$\epsilon_{x,N}^{\rm SR} \approx \frac{55}{32\sqrt{3}} \frac{\lambda\!\!\!^{-}_A}{J_x} \left(\frac{\gamma^3}{Q_\beta^3} \right) \left(\frac{C}{2\pi\rho} \right)^3$$

for LHC-II and HF VLHC 2–3 orders of magnitude below desired design emittance!

→ *large beam-beam tune shifts, halo, background,...?*
(J. Gareyte)

equilibrium emittance determined by balance of radiation damping and **intrabeam scattering**

$$\frac{1}{\tau_{\mathbf{x},\mathrm{IBS}}} \approx \frac{\mathbf{c r_p^2 N_b L_c}}{\mathbf{16 Q} \epsilon_{\mathbf{x,N}}^{\mathbf{2}} \sqrt{\kappa}\sqrt{\kappa+\mathbf{1}}\gamma\sigma_{\mathbf{z}}\sigma_\delta} \quad \text{[J. Wei]}$$

where $L_c \approx 20$. Asymptotically, for $\gamma \gg Q_\beta$:

$1/\tau_{\delta,\mathrm{IBS}} \approx 1/\tau_{x,\mathrm{IBS}}$ and $\sigma_\delta \approx Q_\beta^{3/2}\sqrt{\epsilon_x/\rho}$

IBS equilibrium emittance:

$$\epsilon_{\mathbf{x,N}}^{\mathrm{IBS}} = \frac{\rho^{\mathbf{5/6}}\mathbf{N_b^{1/3}}}{\mathbf{Q}_\beta\gamma^{\mathbf{7/6}}}\left(\frac{\mathbf{Z f_{rf} e V_{rf}}}{\mathbf{cE}\kappa(\kappa+\mathbf{1})}\right)^{\mathbf{1/6}}\left(\frac{\mathbf{C}}{\mathbf{2}\pi\rho}\right)^{\mathbf{1/6}}\left(\frac{\mathbf{3 r_p L_c}}{\mathbf{16}}\right)^{\mathbf{1/3}}$$

f_{rf}: rf frequency; V_{rf}: total rf voltage

$\epsilon_y = \kappa\epsilon_x$ due to coupling and spurious D;
assume $\kappa = 1$ for LHC-II

simulation with SR damping, IBS, particle consumption

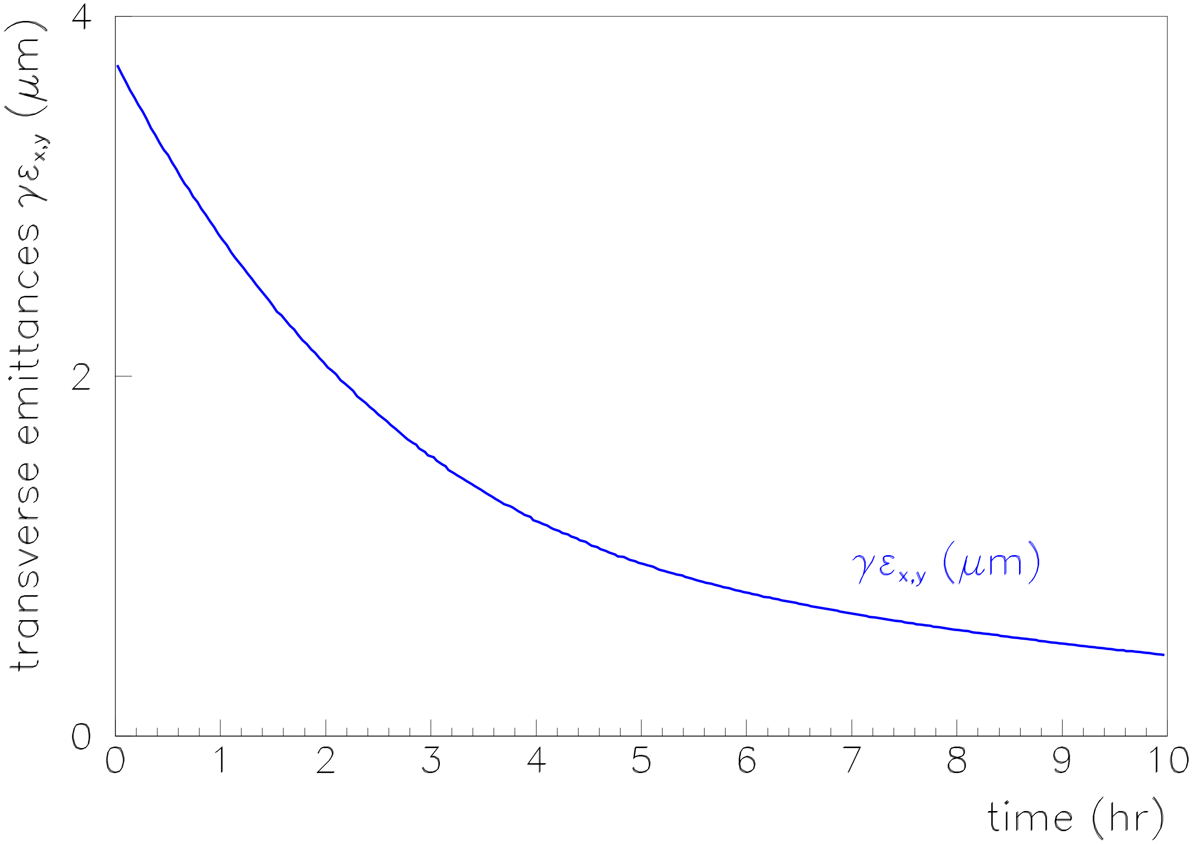

Evolution of **transverse emittance** vs. time in LHC-II.

simulation with SR damping, IBS, particle consumption

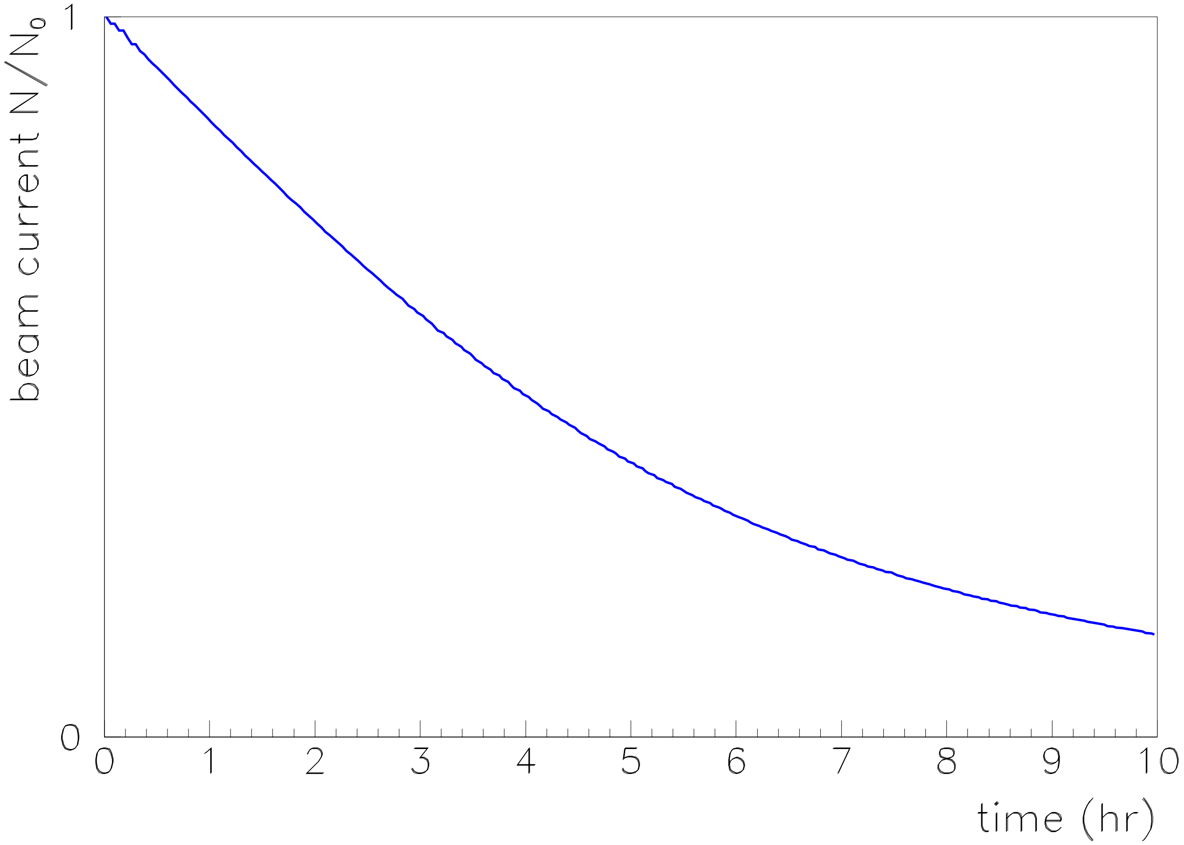

Evolution of **beam current** during a store in LHC-II.

simulation with SR damping, IBS, particle consumption

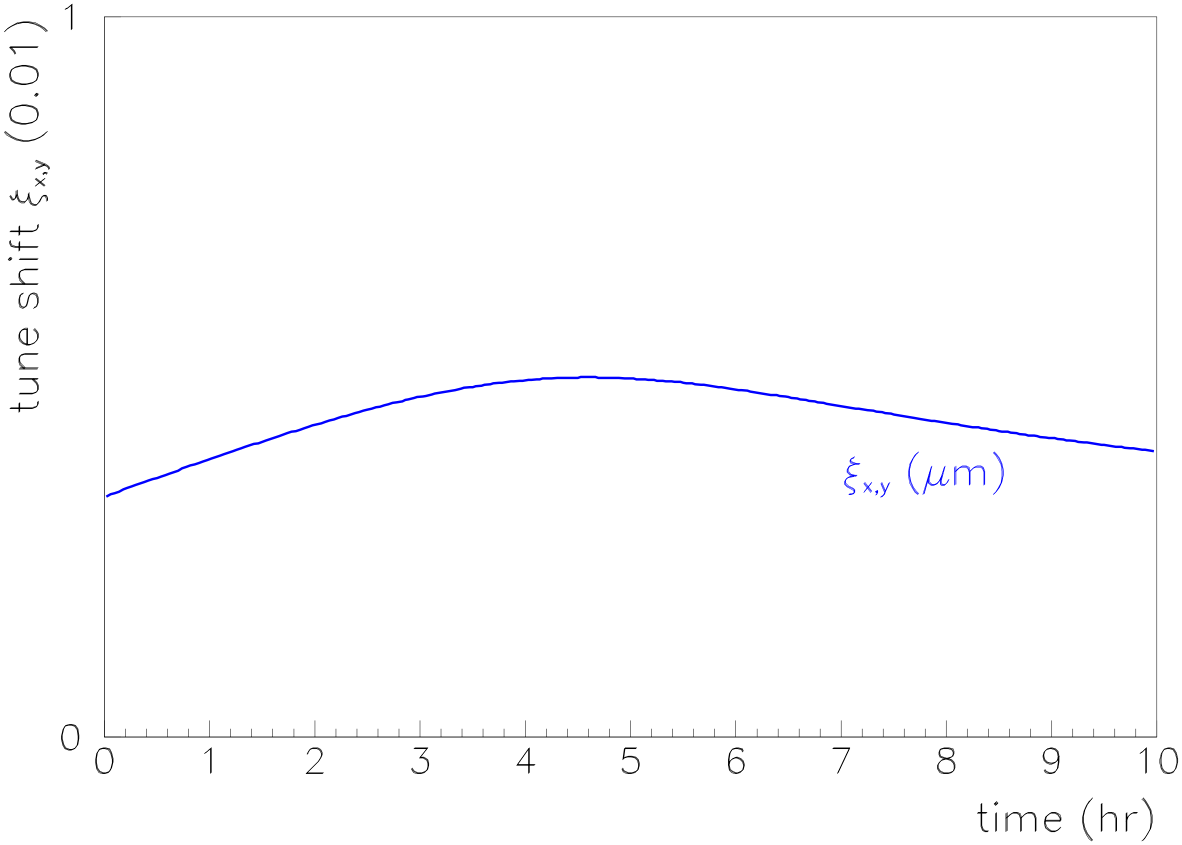

Evolution of **beam-beam tune shift** vs. time in LHC-II.

simulation with SR damping, IBS, particle consumption

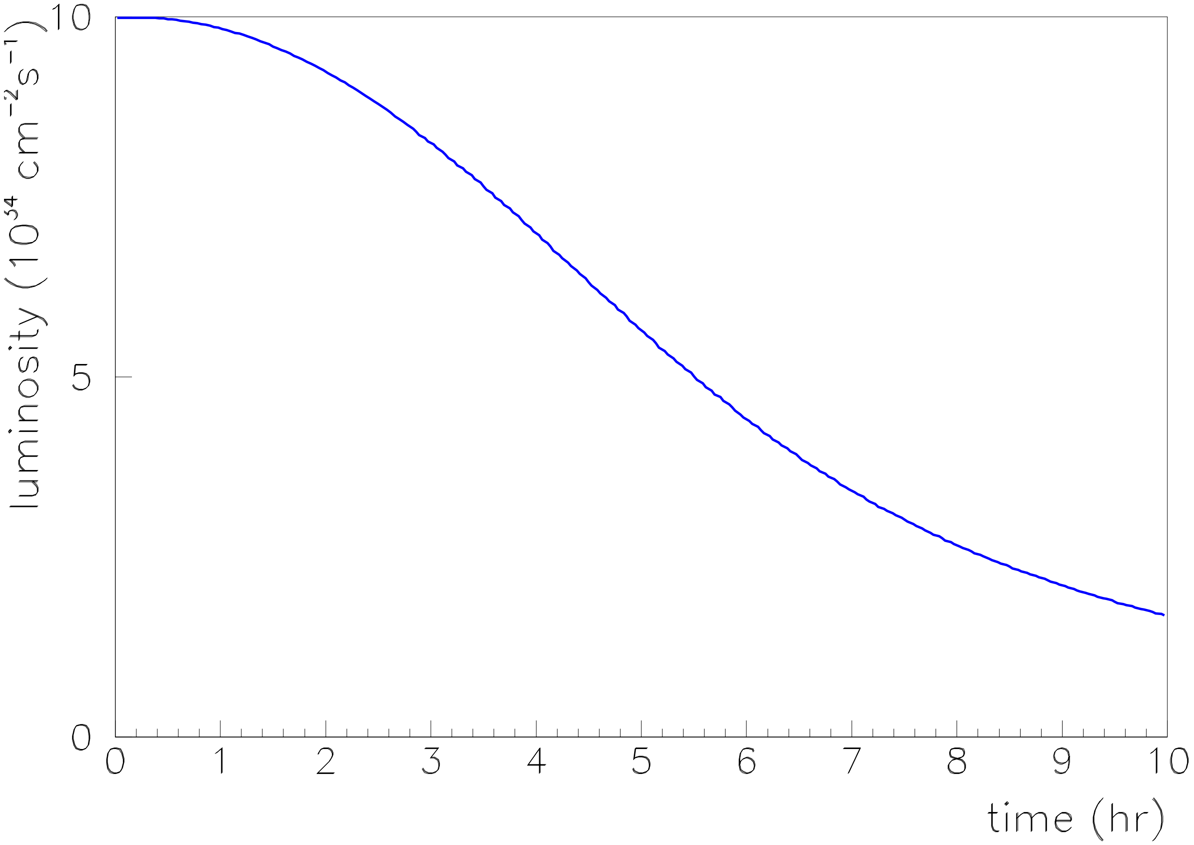

Evolution of **luminosity** during a store in LHC-II.

Collective Effects

- loss of Landau damping for higher-order longitudinal modes (F. Ruggiero, J. Rogers):

$$\sigma_s \geq \frac{C}{2\pi}\left[\frac{\pi^3}{6}\frac{N_b f_{\rm rev} e}{h_{\rm rf}^3 V_{\rm rf}}\ {\rm Im}\left(\frac{Z_L}{n}\right)_{\rm eff}\right]^{1/5}$$

- longitudinal microwave instability
- transverse coupled-bunch resistive-wall instability
- electron cloud

simulation with SR damping, IBS, particle consumption

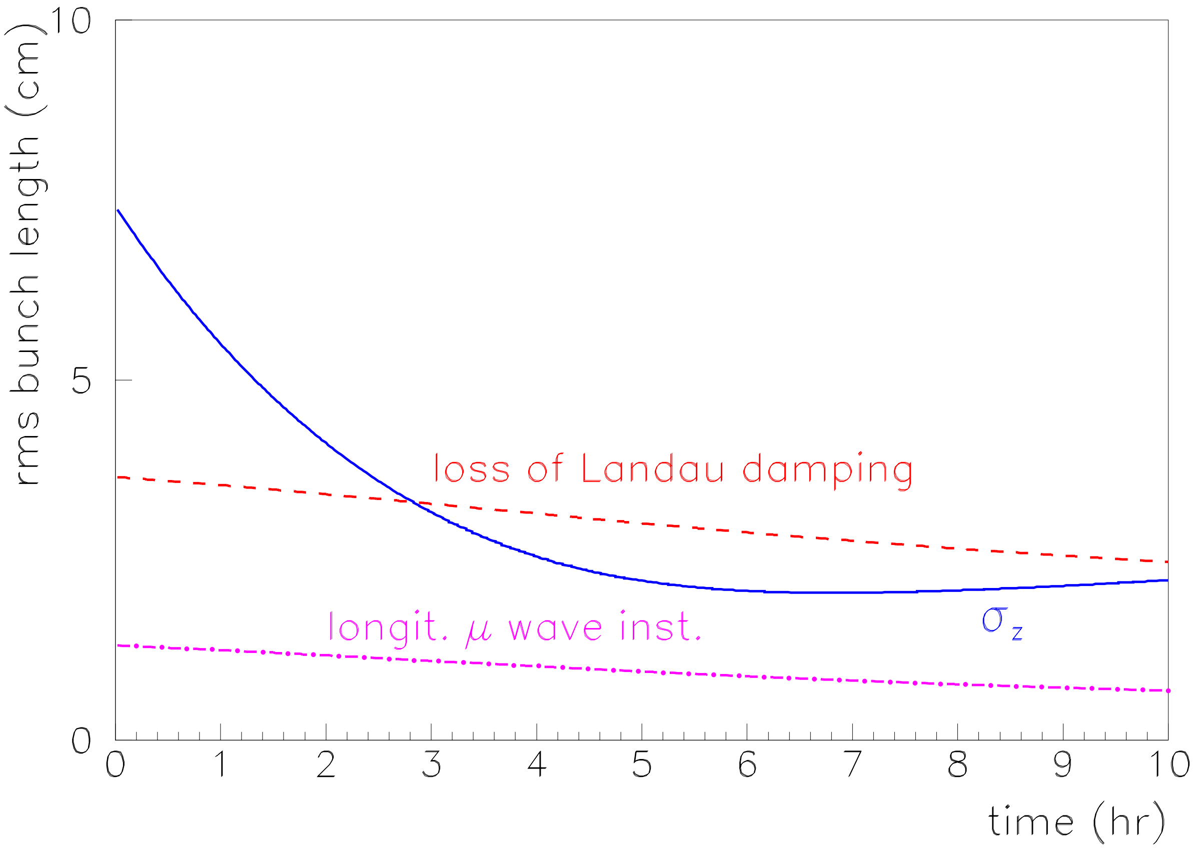

Evolution of **rms bunch length** during a store in LHC-II, and instability thresholds for $\mathrm{Im}(Z_L/n)_{\mathrm{eff}} \approx 0.1\ \Omega$ (LHC).

simulation with SR damping, IBS, particle consumption

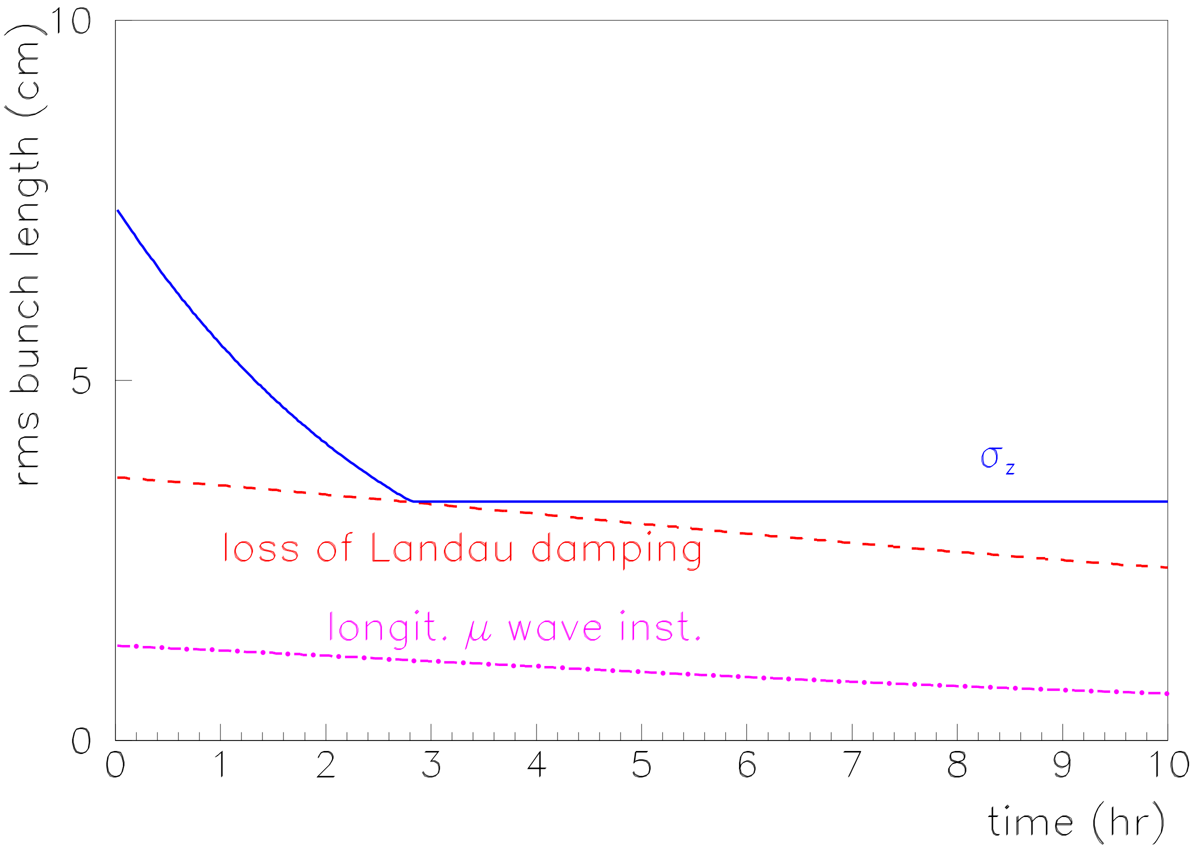

Evolution of **rms bunch length** during a store in LHC-II, when after 3 hours **noise** maintains $\epsilon_L \geq 0.104$ eVs.

Total Beam Current

synchrotron radiation power

$$P_{\rm SR} = \frac{C_\gamma E^4 N_b n_b c}{C\rho} = U_0 f_{\rm rev} n_b N_b$$

using L and ξ this can be rewritten as

$$P_{\rm SR} = \left(\frac{8\pi r_p^{3/2}}{\sqrt{3cE_A}}\right) \frac{\kappa}{1+\kappa^2} \frac{E^{3/2} L \beta_x^*}{\xi\sqrt{J_z\tau_z}} \sqrt{\frac{C}{2\pi\rho}}$$

scaling:

$B = \text{constant} \rightarrow J_z\tau_z \propto 1/E$ and $P_{\rm SR} \propto E^2 L$

$B \propto E^{1/2} \rightarrow J_z\tau_z \propto 1/E^2$ and $P_{\rm SR} \propto E^{5/2} L.$

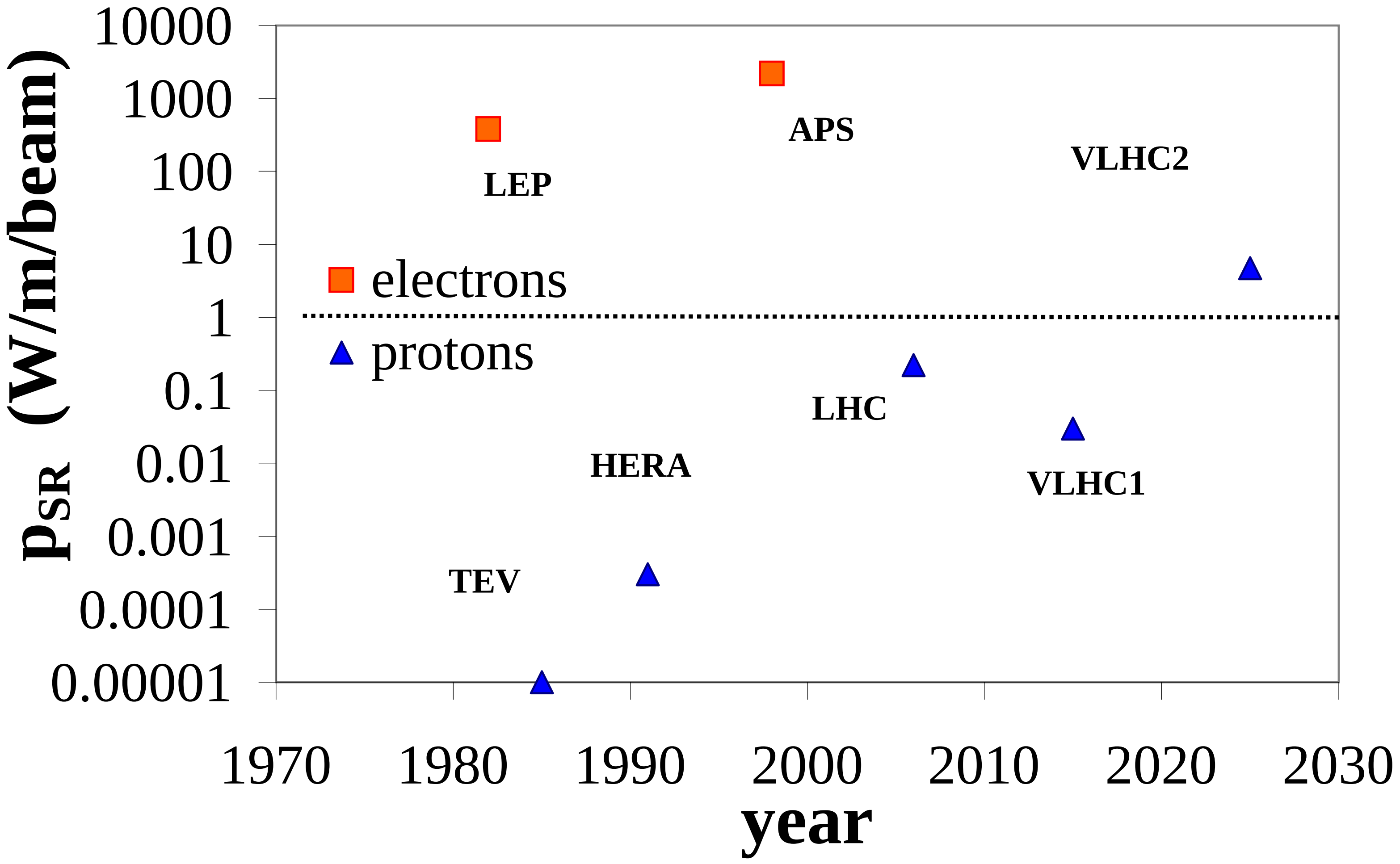

SR power in present and future colliders (P. Bauer et al., PAC2001).

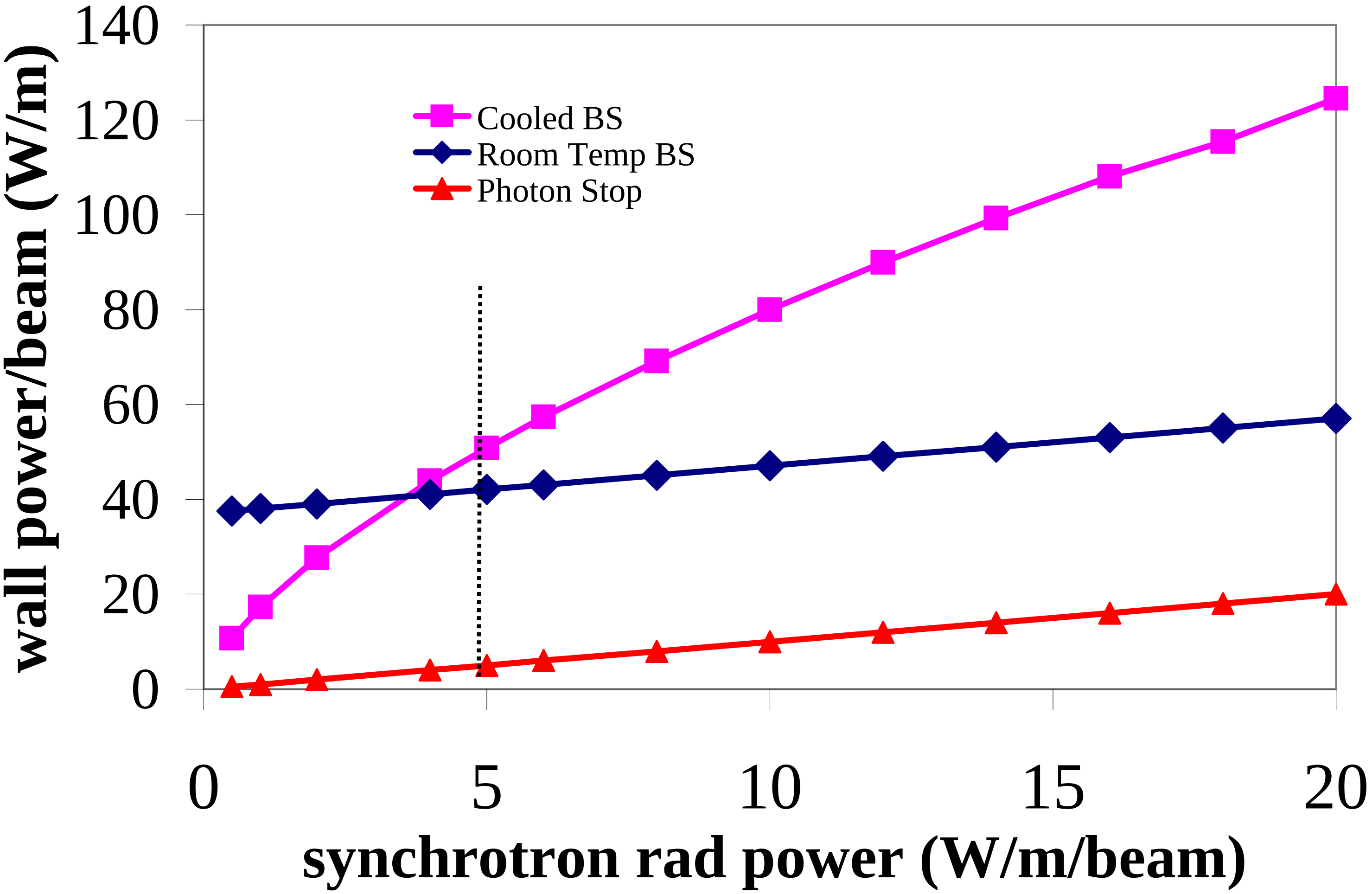

Wall plug power density vs. SR load for different solutions: cold BS, warm BS/shield & photon stop (P. Bauer et al.).

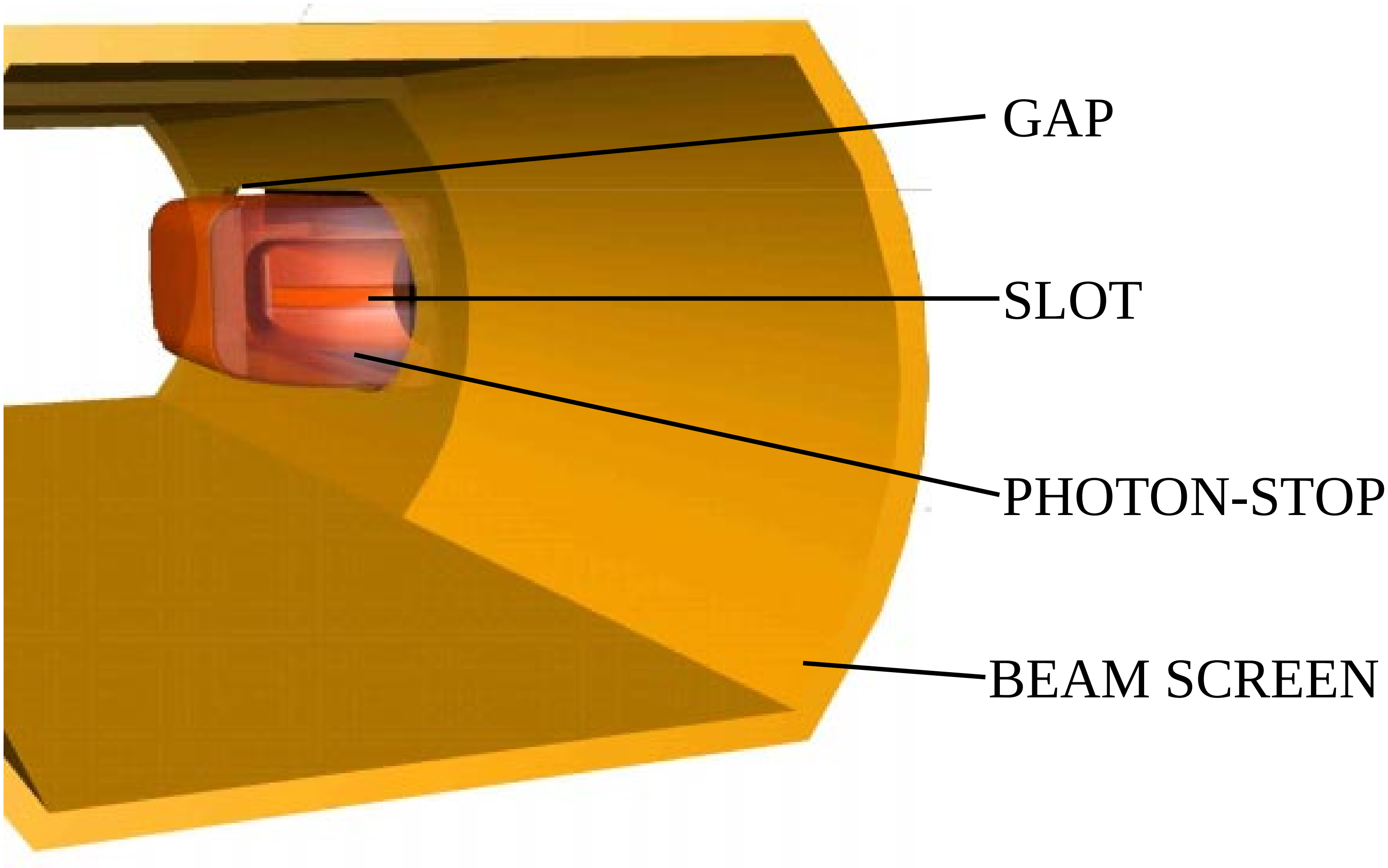

Sketch of the proposed VLHC-II photon stop (P. Bauer et al., PAC2001).

Electron Cloud Heat Load for Shorter Bunch Spacing (LHC Luminosity Upgrade)

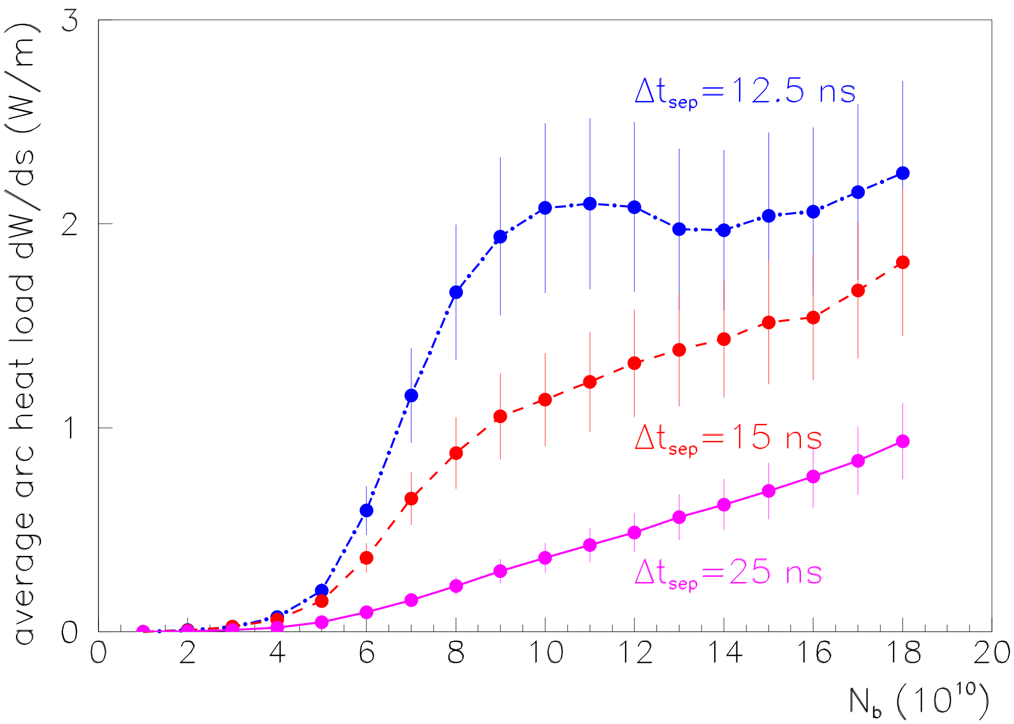

Average arc heat load as a function of bunch population for bunch spacings of 12.5 ns, 15 ns, and 25 ns, and a maximum secondary emission yield $\delta_{\max} = 1.1$. Elastically reflected electrons are included.

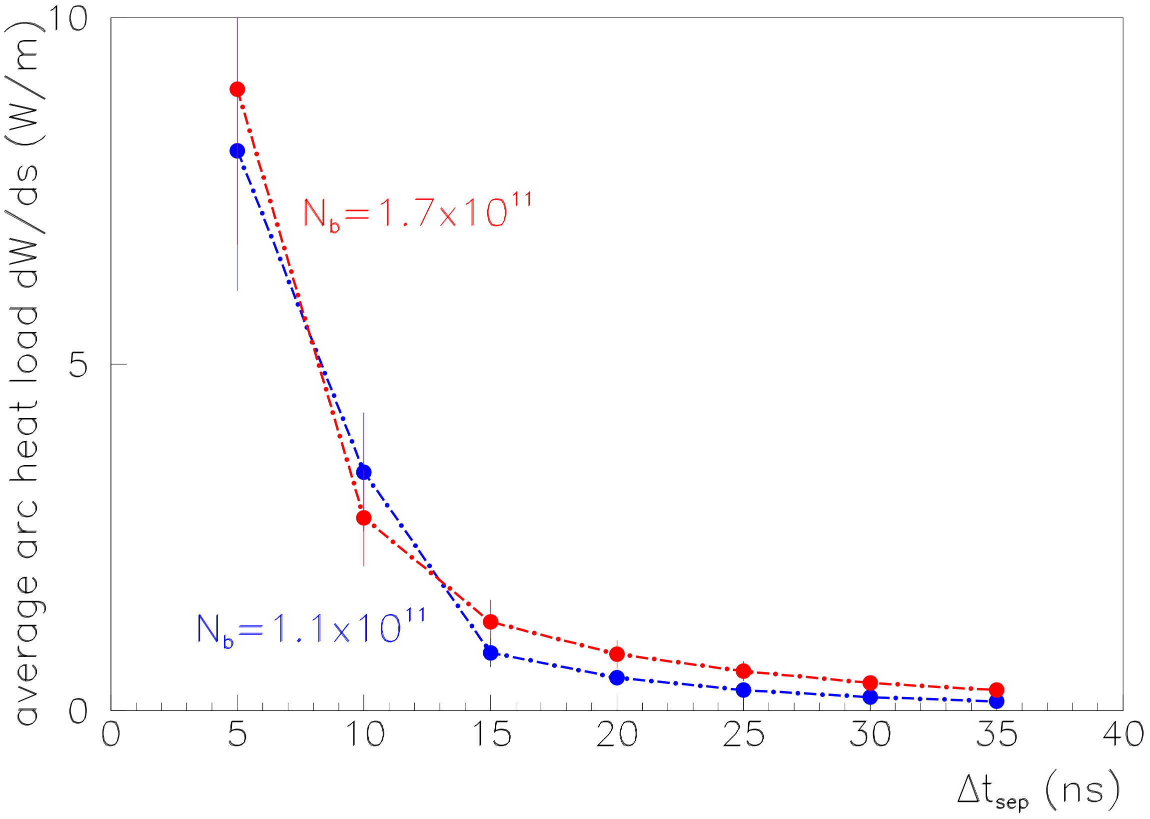

Average arc heat load as a function of bunch spacing, for $\delta_{\max} = 1.1$ and various bunch populations.

Fermilab-TM-2149
June 11, 2001

www.vlhc.org

Design Study for a Staged Very Large Hadron Collider

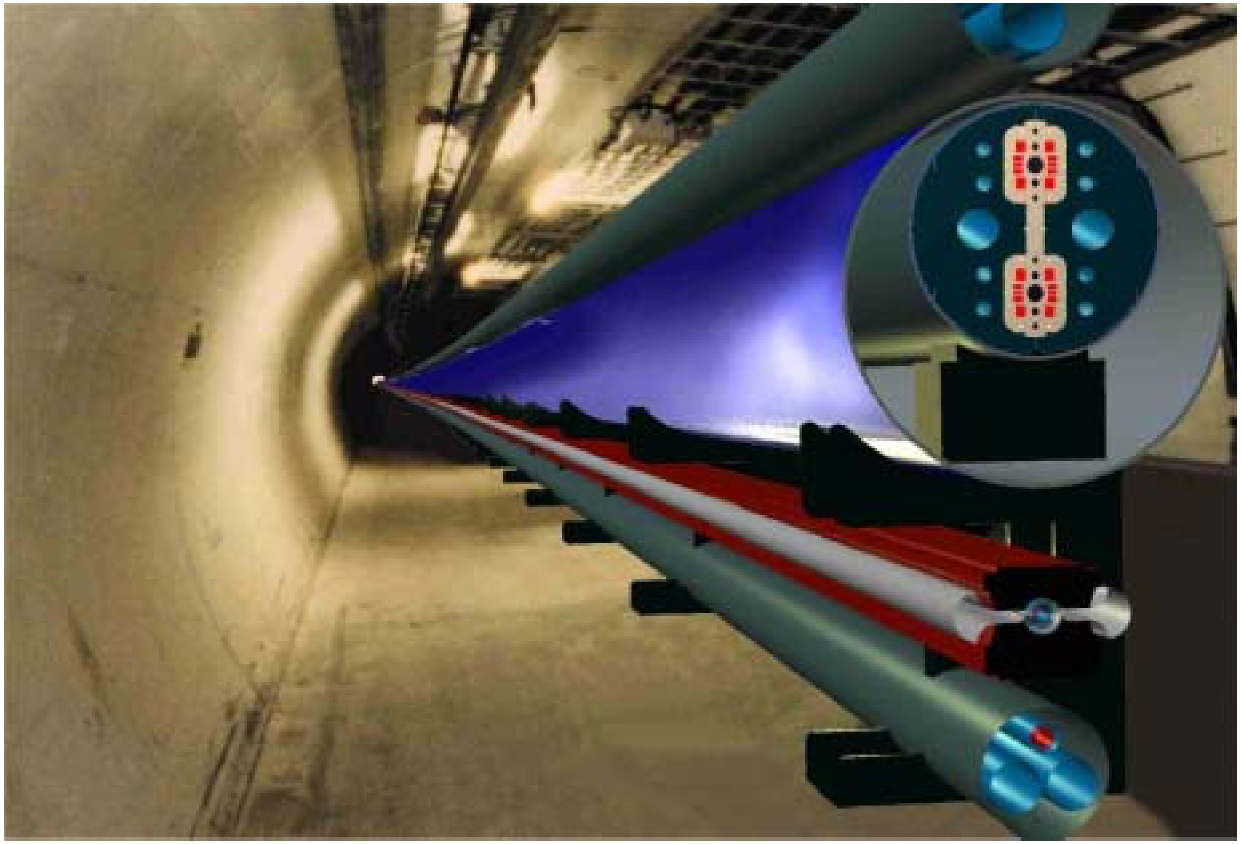

Stage 2 VLHC Tunnel

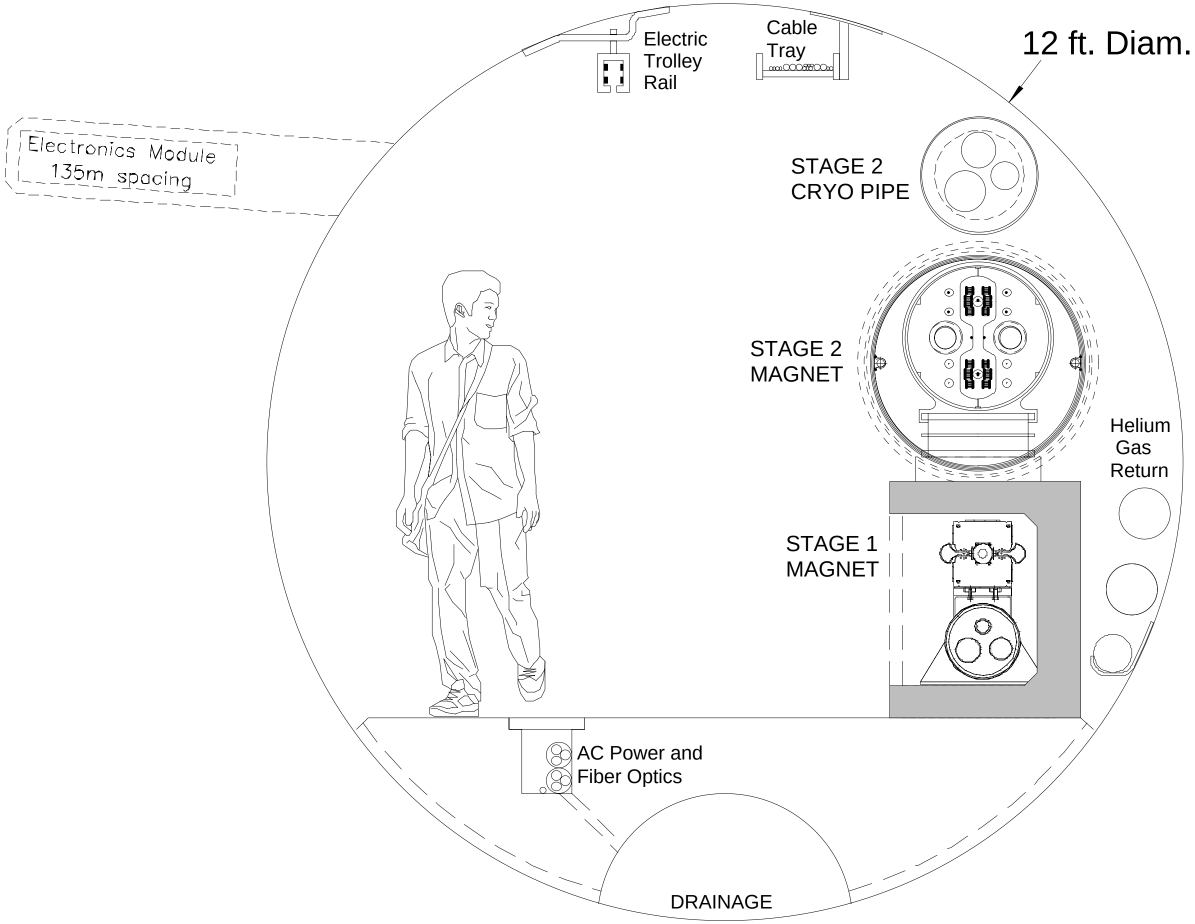

Transmission Line Magnet

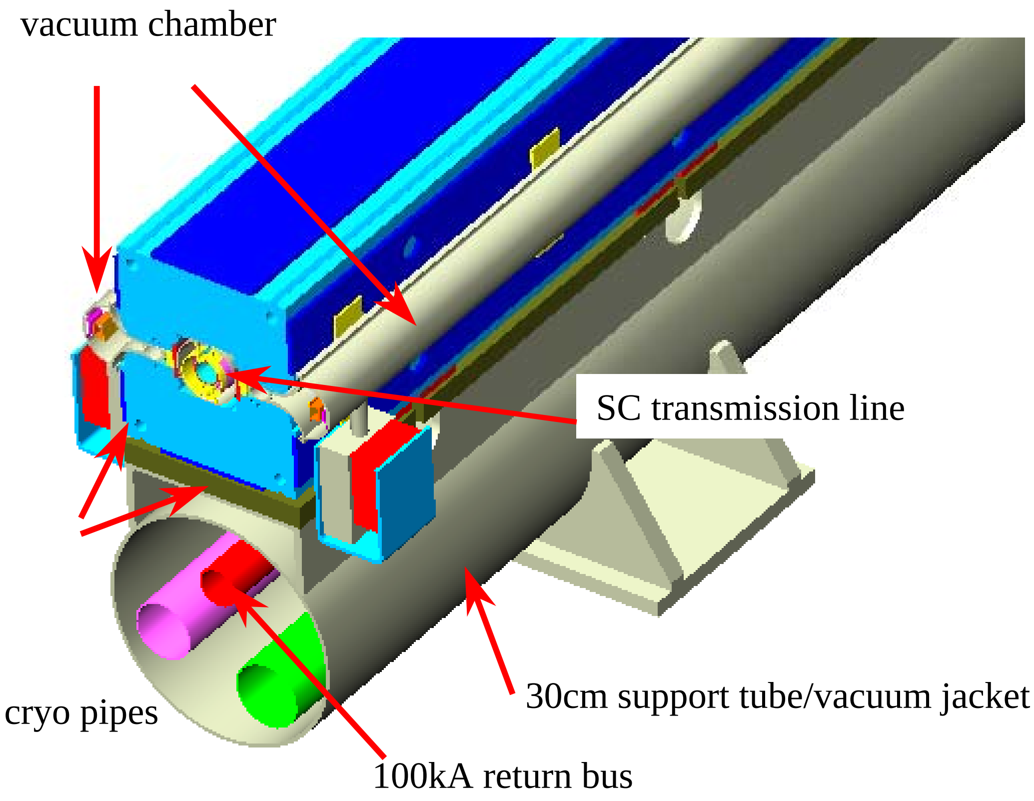

- 2-in-1 warm iron
- Superferric: 2T bend field
- 100kA Transmission Line
- alternating gradient (no quadrupoles needed)
- 65m Length
- Self-contained including Cryogenic System and Electronics Cabling
- Warm Vacuum System

Operating Margin Verified

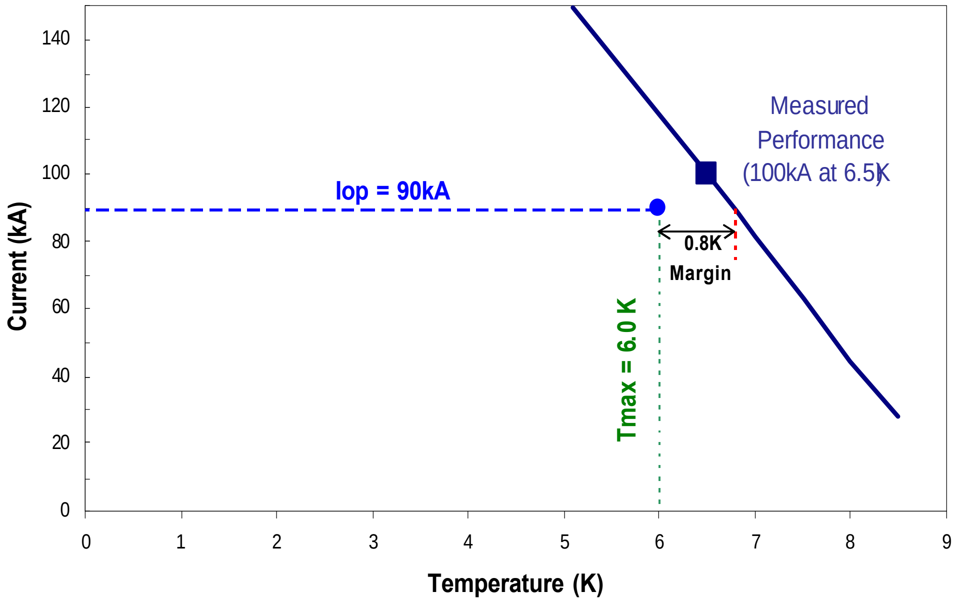

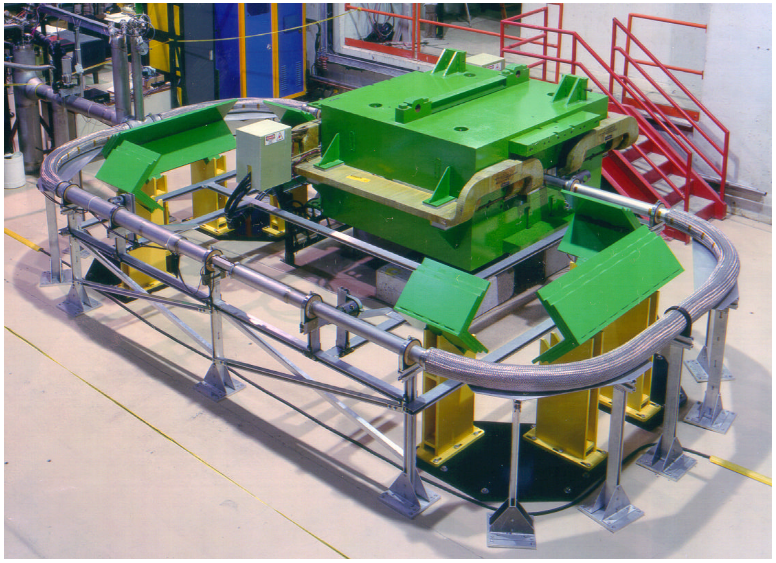

17 meter 100 kA test loop

Seven Designs Tested

~0.8K margin at design current of 87.5 kA

~25kA margin at nominal peak temperature of 6.0 K

(similar margins for three variants used in Design Report)

Very Large Hadron Collider

VLHC DESIGN STUDY SITE LAYOUT

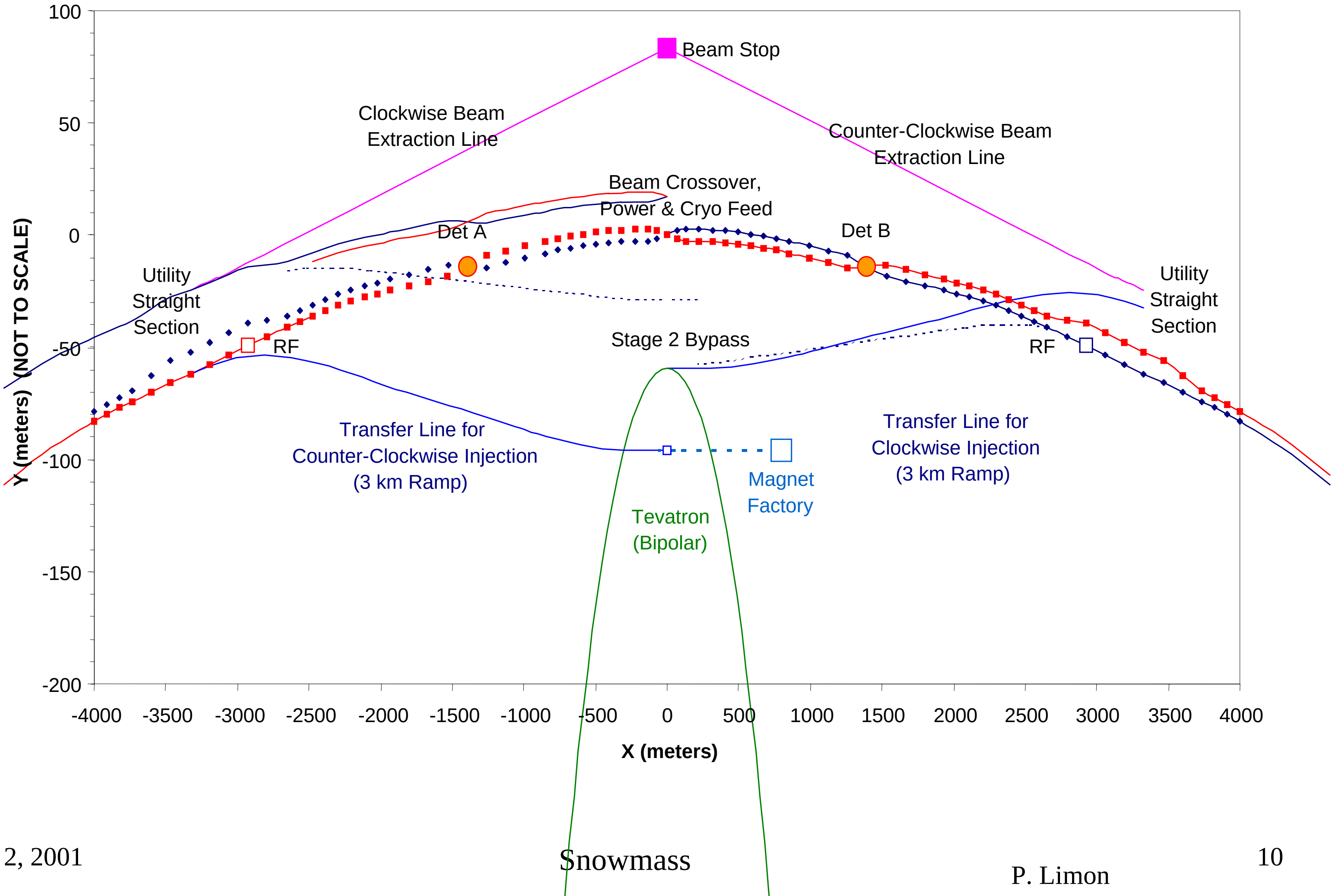

‘Continous Beams’ or Super Bunches

- ISR was extremely successful
- continuous beams abandoned due to scarcity of antiprotons, no longer a problem
- no PACMAN bunches!
- no electron cloud!
- use induction acceleration modules, 25 kV/m, to generate long bunches bounded by barrier buckets (K. Takayama)
- stochastic cooling
- higher current
- route to high luminosity

exciting new development

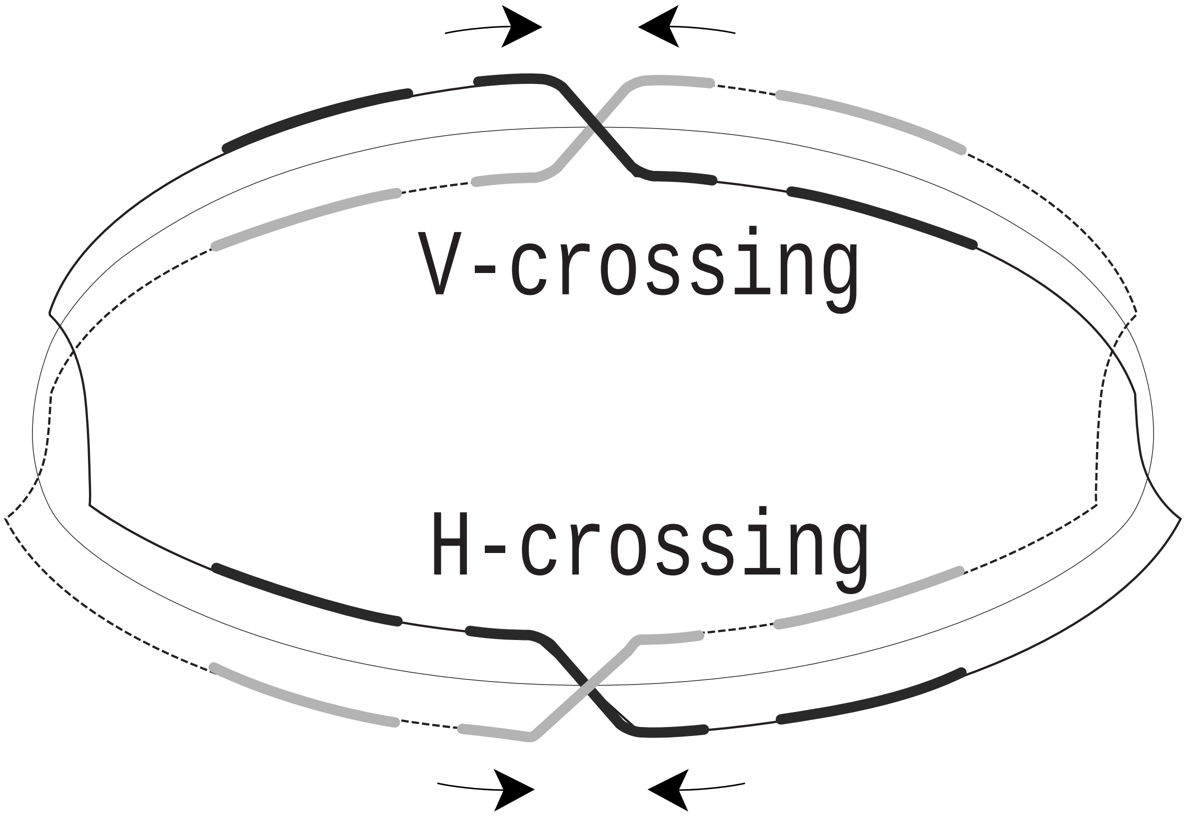

Schematic of Super Bunches in a High-Luminosity Collider
(K. Takayama et al.)

Continuous Beams – Luminosity

$$L = \frac{c\lambda_1\lambda_2 l_{\rm det}}{4\pi\sigma_0^2}\; K\left(\frac{l}{2\beta^*}, \frac{\beta^*\theta_c}{\sigma_0}\right)$$

where

$$K(\xi,\eta) = \frac{1}{\xi}\int_{-\xi}^{\xi} \frac{1}{1+u^2}\exp\left[-\frac{\eta^2}{4}\frac{u^2}{1+u^2}\right]\, du$$

The integral $K(\xi,\eta)$ is defined such that $K(\xi,\eta) \to 2$ for $\xi,\eta \to 0$ (E. Keil, et al., 1972/73).

Continuous Beams – Tune Shift

For horizontal crossing, the beam-beam tune shifts are

$$\Delta Q_x = \frac{2\lambda r_p l}{4\pi\gamma\epsilon_\perp} I_x\left(\frac{l}{2\beta^*}, \frac{\beta^*\theta_c}{\sigma_0}\right)$$

$$\Delta Q_y = \frac{2\lambda r_p l}{4\pi\gamma\epsilon_\perp} I_y\left(\frac{l}{2\beta^*}, \frac{\beta^*\theta_c}{\sigma_0}\right)$$

where

$$I_x(\xi,\eta) = \frac{1}{\xi\eta^2}\int_{-\xi}^{+\xi}(1+u^2)\left[\left(u^{-2}+\frac{\eta^2}{1+u^2}\right)\exp\left(-\frac{\eta^2}{2}\frac{u^2}{1+u^2}\right) - u^{-2}\right] du$$

$$I_y(\xi,\eta) = \frac{1}{\xi\eta^2}\int_{-\xi}^{+\xi}(1+u^{-2})\left[1-\exp\left(-\frac{\eta^2}{2}\frac{u^2}{1+u^2}\right)\right] du$$

and the interaction happens between $-l/2$ and $l/2$. The integrals $I_{x,y}(\xi,\eta)$ are defined such that $I_{x,y}(\xi,\eta) \to 1$ for $\eta \to 0$ and all ξ.

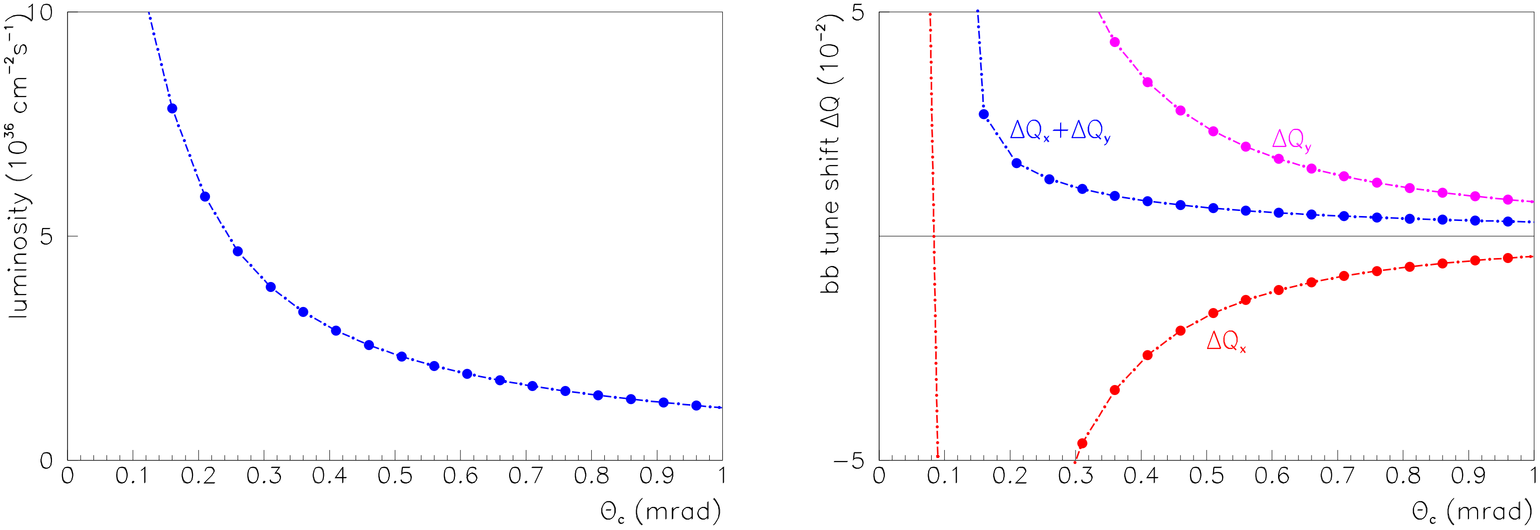

Luminosity (left) and beam-beam tune shifts (right) as a function of crossing angle, for a continuous beam with a line density $\lambda = 8.8 \times 10^{11}$ m^{-1} (40 A current), $\beta^* = 0.25$ m, $l_{\rm det} = 1$ m, $l = 20$ m, and $\gamma\epsilon_\perp = 3.75$ μm.

Optimization of Continuous Beam Parameters – Length & Number & Charge of Super-Bunches?

Ongoing Study at CERN

- maximum luminosity
- maximum beam-beam tune shift
- acceptable heat load
- timing constraints by (induction) rf system
- injectors and filling time
- beam abort system

(D) Conclusions

- hadron colliders have performed exceedingly well in the past
- the LHC will break new territory:
  - highest energy (14 TeV) and highest luminosity (10^{35} cm^{-2}s^{-1}) ever
  - long-range collisions
  - strong-strong collisions
  - electron cloud

  - radiation damping stronger than IBS

- beyond LHC: LHC upgrades and various stages of VLHC, Eloisatron, ...
  - higher fields or larger circumference (→ peculiar collective effects)
  - more synchrotron radiation; possibly more electron cloud
  - new exciting development: ‘quasi-continuous beams’ (closing the circle to the ISR)

Thanks

G. Arduini, R. Assmann, P. Bagley, P. Bauer, F. Bordry, L. Bottura, D. Brandt, O. Brüning, I. Collins, K. Cornelis, A. Faus-Golfe, W. Fischer, J. Gareyte, O. Gröbner, H. Grote, G. Guignard, W. Herr, J.B. Jeanneret, J.M. Jimenez, C. Johnstone, J. Jowett, E. Keil, J.-P. Koutchouk, K.-H. Mess, K. Ohmi, S. Peggs, F. Pilat, L. Rossi, F. Ruggiero, G. Rumolo, F. Schmidt, R. Schmidt, E. Shaposhnikova, V. Shiltsev, M. Syphers, T. Taylor, R. Thomas, A. Verdier, L. Vos, J. Wei,...

Web addresses

- LHC http://lhc.web.cern.ch/lhc/
- LHC beam-beam effects http://wwwslap.cern.ch/collective/zwe/lhcbb/Welcome.html
- LHC electron cloud http://wwwslap.cern.ch/collective/electron-cloud/electron-cloud.html

- Accelerator Physics Group of the CERN SL (SPC+LHC) Division http://wwwslap.cern.ch/
- VLHC http://vlhc.org/

Extended Parameter Set for pp or p$\bar{\text{p}}$ Colliders x

acc.	Sp$\bar{\text{p}}$S	TeV2a	LHC	LHC-II	VLHC-I	VLHC-II
E [TeV]	0.32	0.98	7	14	20	87.5
B [T]	1.4	4.34	8.4	16.8	2	9.8
$\frac{\text{energy}}{\text{beam}}$ [MJ]	0.05	1	334	1320	3328	4200
C [km]	6.9	6.28	26.7	26.7	233	233
n_b	6	36	2800	5600	40000	40000
N_b [10^{11}]	1.7 (p) 0.8 ($\bar{p}$)	2.7 (p) $\sim$1.0 ($\bar{p}$)	1.05	1.05	0.26	0.075
$\hat{L}$ [$\frac{1}{10^{34}\text{cm}^{-2}\text{s}^{-1}}$]	0.0006	$\sim$ 0.02	1.00	10.	1.0	2.0
$\sigma^*_{x,y}$ [μm]	80, 40	32	15.9	7.4*	4.6	3.4 →0.79
$\sigma^*_{x',y'}$ [μrad]	136, 272	91	31.7	34*	15	5 →1

acc.	$\mathrm{Sp\bar{p}S}$	TeV2a	LHC	LHC-II	VLHC-I	VLHC-
$\beta^*_{x,y}$ [m]	0.6, 0.15	0.35	0.5	0.22	0.3	0.71
no. of IPs	3	2	2 (4)	2 (4)	2	2
bb t.-s./IP $\xi_{x,y}$	0.005	0.01	0.0034	0.003↔0.005	0.002	→0.00
θ_c [μrad]	0	0	300	300	153	10
σ_z [cm]	30	37	7.7	4.0	3.0	→1.5
$L_{\rm sep}$ [m]	1150	119	7.48	3.74	5.645	5.645
$P_{\rm SR}$ [kW]		$< 10^{-3}$	3.6	114	7	1095
dP/ds [W/m]		$\ll 10^{-3}$	0.2	6.6	0.03	4.7
$\tau_{\rm IBS}$ [hr]	10	50(?)	142	345 (in.)	400	4000→1
$\tau_{y,{\rm SR}}$ [hr]		1200	52	6.5	200	2
d.d./IP δ [10^{-10}]		0.025	2.5	20	5	400
events/cross.		~6	18	90	21	54

acc.	Sp$\bar{p}$S	TeV2a	LHC	LHC-II	VLHC-I	VLHC-II
lum. lifet. τ_L [hr]	9	9	10	3.2	24	8
tune Q_β	26	∼20	63	63	220	220
$\gamma\epsilon_{x,y}$ [μm]	3.75	~ 3	3.75	3.75→1.0	1.5	1.6→0.04
$\gamma\epsilon_x^{eq}$ [μm]		$\sim 10^\star$	2.03	1.07	1.0	0.06
ϵ_L (σ) [eVs]	0.11	0.11	0.2	→0.15	0.4	0.4 →0.1